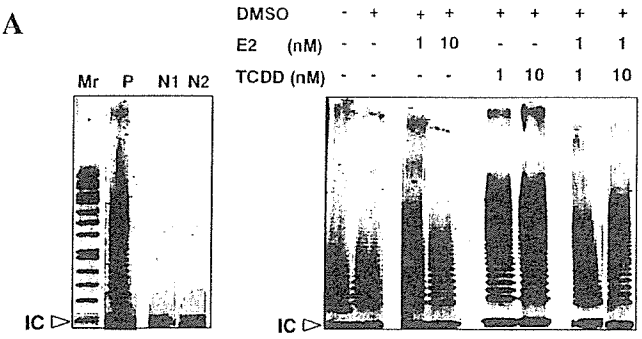

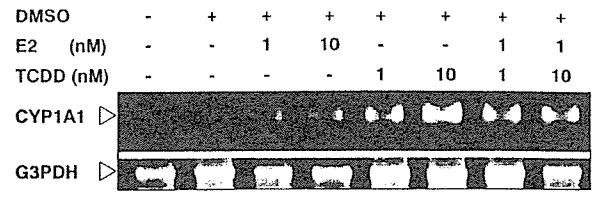

Figure 2. E2, TCDD or a combination of the two induces *CYP1A1* expression in BeWo cells. Cells were treated with E2, TCDD alone or a combination of the two for 24 h at different dose concentrations. DMSO was used as vehicle control. RT-PCR was performed using *CYP1A1*-specific primers and 10 μl of each reaction was resolved in a 1.5% agarose gel and visualized by ethidium bromide staining. G3PDH was used as the internal control.

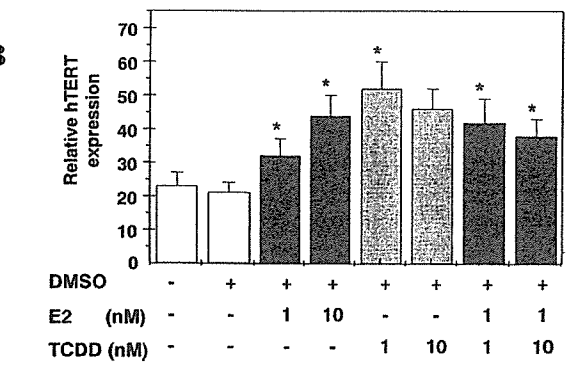

Figure 1. E2 and TCDD induce telomerase activity and hTERT expression in BeWo cells. Cells were treated for 24 h with E2 (1- and 10-nM), TCDD (1- and 10-nM) and a combination of 1-nM E2 with both 1- and 10-nM of TCDD. (A) Telomerase activity was measured by stretch PCR assay. The data shown are the results of one of three independent experiments performed in triplicate. Telomerase activity in HeLa cell extracts was used as a positive control (P), and lysis buffer only (N1) and cell extracts treated with RNase (N2) were used as negative controls. The activity of telomerase in BeWo cell extracts is shown without any treatment, with DMSO, 1- and 10-nM E2, 1- and 10-nM TCDD, 1-nM E2 with 1-nM TCDD, and 1-nM E2 with 10-nM TCDD. Mr, molecular weight markers; IC, internal control. (B) hTERT activity in BeWo cells following the indicated treatments for 24 h. hTERT induction was determined by real-time PCR. Values are the mean ± SD of three different cDNAs, each from one experiment. Triplicate experiments gave similar results.

in buffer containing 50 mM Tris-HCl (pH 7.5), 140 mM NaCl, 10% glycerol, 1% Nonidet P-40, 100 mM NaF, 200 mM Na_3VO_4, 1 mM phenylmethysulfonyl fluoride, 10 μg/ml leupeptin, 10 μg/ml aprotinin and 10 μg/ml chymotrypsin. The lysates were centrifuged at 15000 rpm for 15 min at 4°C and the protein concentrations in supernatant were determined using a BioRad kit (BioRad). Approximately 50 μg of total cell lysate was denatured in SDS containing sample buffer (BioRad) by boiling at 100°c for 2 min. Proteins were separated on 10% SDS-PAGE and transferred to PVDF nylon membrane using a semi-dry transfer apparatus (BioRad). The membrane was blocked in 5% skimmed milk in Tris-HCl buffer, pH 7.5 for 1 h and then incubated with c-Myc antibody (C-19:sc-788; Santa Cruz Biotechnology, Santa Cruz, CA) at a dilution of 1:200 for 1 h at room temperature in the same buffer. The c-Myc-specific band was detected by incubating the membrane for 1 h with anti-rabbit alkaline phosphatase-conjugated secondary antibody followed by detection with the NBT/BCIP substrate.

Immunofluorescent staining of c-Myc. Cells were grown on sterile glass coverslips and then treated with E2, TCDD or both in the presence of 10% charcoal-stripped serum for 24 h. After this period, the cells were washed with chilled PBS and fixed with cold methanol for 20 min at -20°C. The cells were then washed again and further blocked with 5% normal goat serum for 1 h at room temperature, followed by another 1 h incubation with c-Myc antibody (sc-788, Santa Cruz Biotechnology) at a dilution of 1:200 in PBS with 5% goat serum. The cells were then washed three times with PBS and incubated with anti-rabbit rhodamine-conjugated secondary antibody (Santa Cruz Biotechnology) at a dilution of 1:200 for 1 h. Finally, the cells were washed with PBS followed by incubation with 4, 6-diamino-2-phenylindole (DAPI) for 5 min and then thoroughly washed again with PBS. After this, the coverslips were placed on glass slides under glycerol and viewed under a UV-microscope (Leica, Cologne, Germany).

Results

Upregulation of telomerase activity and the mRNA expression of hTERT and CYP1A1. Telomerase activity in BeWo cells was determined by assaying telomere repeat lengths and telomerase catalytic subunit expression (Fig. 1). BeWo cells treated with both 1- and 10-nM of E2 for 24 h had significantly increased telomerase activity levels when compared to DMSO control-treated cells and 1-nM E2 treatment resulted in significantly higher telomerase activity than the 10-nM dosage. BeWo cells treated with TCDD at 1- and 10-nM concentrations showed a dose-dependent increase in telomerase activity. In contrast, when these cells were co-treated with 1-nM E2, they showed a marginal decrease in telomerase activity when compared to TCDD alone. Since treatment with 1-nM E2 induced the highest level of telomerase activity, this concentration was used in additional co-treatment studies with TCDD.

Among the various components that have been shown to be associated with the telomerase complex, the telomerase catalytic subunit, hTERT, has been demonstrated to be the rate-limiting determinant of telomerase activity (33). hTERT expression levels were, therefore, examined to establish whether telomerase activation by E2 and TCDD was indeed mediated through activation of the catalytic subunit. As shown in Fig. 1B, the levels of hTERT mRNA showed significant increases following E2 and TCDD treatment when compared to both the DMSO-untreated and -treated cells. Activation of

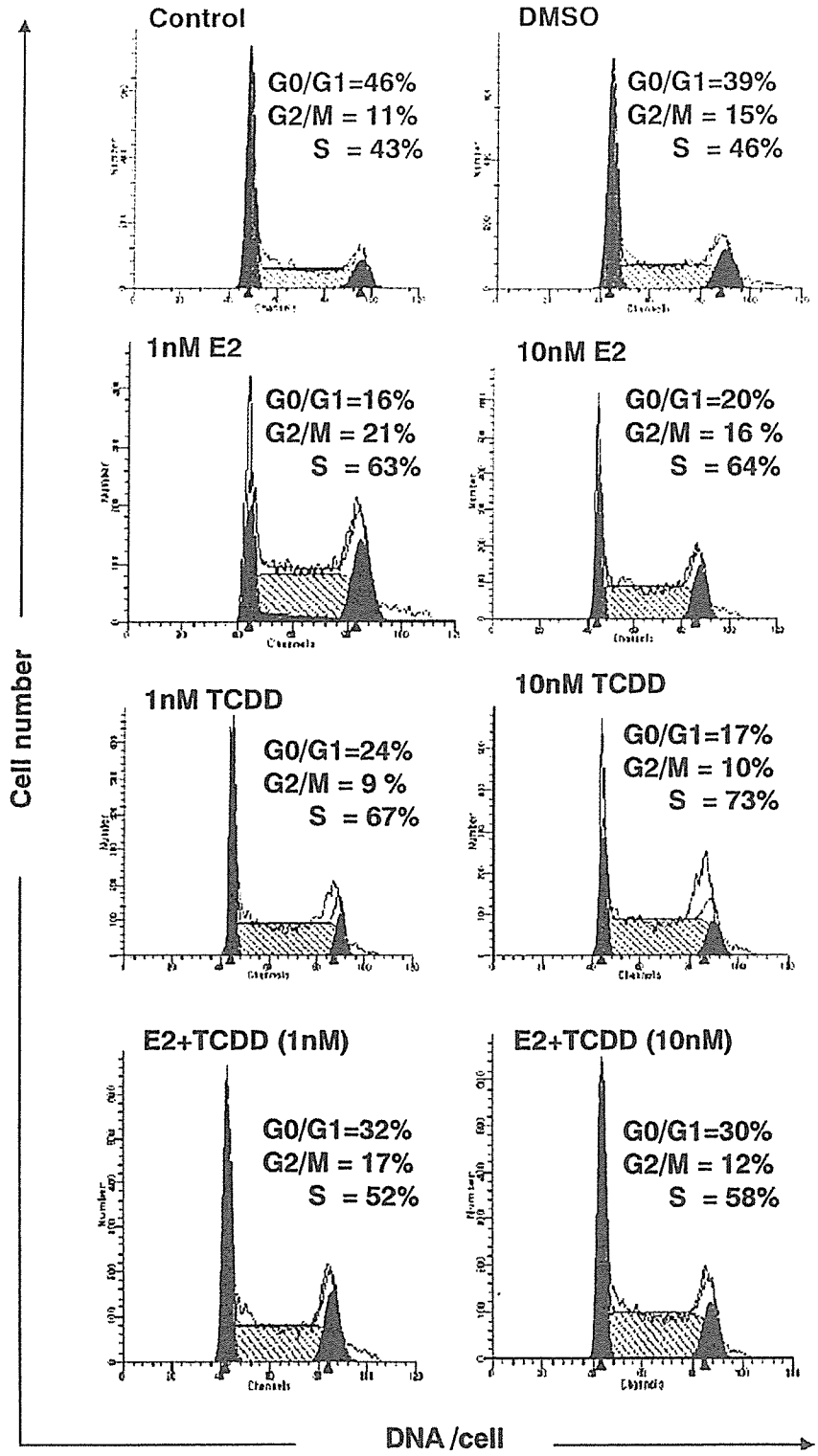

Figure 3. Representative flow cytometric data of effects of E2 and TCDD on BeWo cells. The first peak (left, red) indicates the percentage of cells in G1/G0-phase, the middle peak (blue, diagonal) indicates the percentage of cells in S-phase and the third peak (right, red) indicates the percentage of cells in G2-phase. BeWo cells were serum-starved for 24 h, treated with either E2, TCDD or both in the presence of 10% charcoal-stripped serum, and grown for 24 h prior to being harvested. The cells were then fixed with ethanol and stained with propidium iodide.

hTERT has been shown to be mediated by ER and, therefore, there was a significant increase in hTERT copy number, concomitant with increased telomerase activity, at both concentrations of E2 (1- and 10-nM). TCDD at 1- and 10-nM concentrations also significantly increased the hTERT copy number, which also effectively increased telomerase activity levels. In the presence of 1-nM E2, however, TCDD treatment resulted in a marginal decrease in telomerase activity when compared to treatment with TCDD alone.

Induction of *CYP1A1* is a known marker for the effect of TCDD in most cells examined so far and, therefore, to confirm the action of TCDD in BeWo cells, *CYP1A1* gene expression levels were analyzed by RT-PCR (Fig. 2). TCDD treatment indeed induced *CYP1A1* in a dose-dependent manner. E2

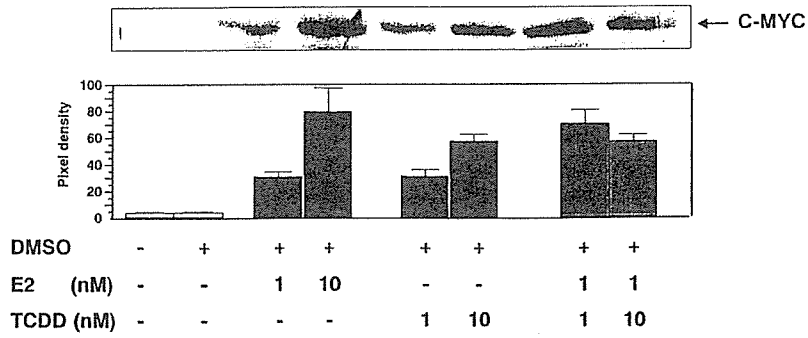

Figure 4. Induction of c-Myc by E2 and TCDD in BeWo cells. The cells were treated with agents for 24 h as described in Fig. 1 and were then harvested. Total cell lysate (50 μg) was resolved by 12% SDS-PAGE and the proteins were transferred to PVDF membranes followed by immunoblotting analysis using c-Myc specific antibodies. This was followed by incubation with an alkaline-phosphatase conjugated secondary antibody and the specific bands were then visualized by BCIP/NBT staining. Picture data are from a representative experiment of three. Graphs are displayed as pixel density of the average of each band ± SD (n=3).

treatment alone resulted in only marginal induction of *CYP1A1*. The combination of both did not show any additive or synergic effects. These results confirm that E2 and TCDD induce *CYP1A1* in BeWo cells.

E2 and TCDD increase DNA synthesis in BeWo cells and the role of c-Myc. The cells were synchronized by serum starvation for 24 h and then treated with E2, TCDD or both in the presence of 10% charcoal-stripped serum for a further 24 h (Fig. 3). Among the cells treated with 1- and 10-nM E2 concentrations, the proportion of cells in S-phase were 63 and 64%, respectively; the corresponding percentages with the same concentrations of TCDD were 67 and 73%, respectively. The increase in the number of cells in S-phase, following E2 and TCDD treatment, suggests that the cells have a higher tendency towards proliferation, which is consistent with previous results showing the association of telomerase activity with cellular proliferation (34). However, following co-treatment with both E2 (1nM) and TCDD, the proportion of cells in S-phase was reduced to 52 and 58%, at 1- and 10-nM TCDD doses, respectively. Thus, TCDD-induced cell proliferation was decreased in the presence of E2, compared to TCDD alone.

c-Myc acts as a positive transcriptional activator of hTERT as the *hTERT* core promoter contains two c-Myc binding sites (35). E2 has been shown to activate c-Myc in MCF-7 cells, resulting in increased cellular proliferation and in the up-regulation of telomerase activity (19). To determine whether the activation of c-Myc is also involved in telomerase activation by TCDD, BeWo cells were treated for 24 h with E2 and TCDD and total cell lysates were subjected to Western blot analysis. Results from this analysis showed that there was significant induction of c-Myc by both E2 and TCDD, at concentrations of both 1- and 10-nM, in a dose-dependent manner (Fig. 4). Additionally, co-treatment of 1-nM E2 with either 1- or 10-nM TCDD induced significantly higher levels of c-Myc, compared to 1-nM E2 treatment alone but, in the presence of both E2 and TCDD, at dose concentrations of 10-nM, there was marginally less induction, suggesting that there was an antagonistic relationship between the two stimulants.

Expression of c-Myc has been closely associated with cellular proliferation and hTERT activity, which is consistent with the induction of c-Myc by TCDD and the resulting increase in telomerase activity. To further confirm the increased levels and the localization of c-Myc expression in BeWo cells, immunostaining was performed in cells treated with either E2 and TCDD, or both (Fig. 5). In control cells, no c-Myc staining was observed, whereas clear nuclear staining of c-Myc was evident following E2 treatment at a concentration of 1-nM and also following TCDD treatment at both 1- and 10-nM concentrations. Nuclear c-Myc staining in cells treated with 1-nM TCDD was slightly defuse but was intense at 10-nM TCDD doses. The nuclear staining pattern at 1-nM E2 and 1-nM TCDD was more defuse and of lower intensity than at the co-treatment with 1-nM E2 and 10-nM TCDD. These results clearly indicate that c-Myc is induced by both E2 and TCDD and that the translocation of the c-Myc protein was not disrupted in the presence of these agents.

Telomerase activation of TCDD depends on c-Myc expression. To confirm that the activation of telomerase by TCDD is c-Myc dependent, HO15.19 cells (Myc-/-) and their parental cells, the TGR-1 cells (Myc+/+) (36), were treated with TCDD for 24 h. Neither of these cell lines expressed ER, as determined by RT-PCR (data not shown), which was consistent with earlier observations (37). In the present study, it was necessary to determine the presence of AhR and ARNT in these cells since TCDD-induced cellular events are mostly mediated through the binding of AhR and the association with ARNT. Semi-quantitative RT-PCR showed that treatments with 1- or 10-nM TCDD did not increase mRNA expression levels of AhR and ARNT while the expression of AhR and ARNT was detected at steady state levels in both cell lines (Fig. 6). *CYP1A1* expression was not induced by TCDD treatment in these cells (data not shown). This lack of induction is consistent with the previous findings that the presence of functional ER is essential in TCDD-induced *CYP1A1* expression (14,18).

To investigate the telomerase activity, both rat cell lines were subsequently treated with E2 (1-nM) and TCDD (10-nM) for 24 h (Fig. 7). The results showed that telomerase activity was absent in HO15.19 cells, even following treatment with E2 and TCDD (Fig. 7, left panel). A significant increase in telomerase activity, however, was observed in TGR-1 cells

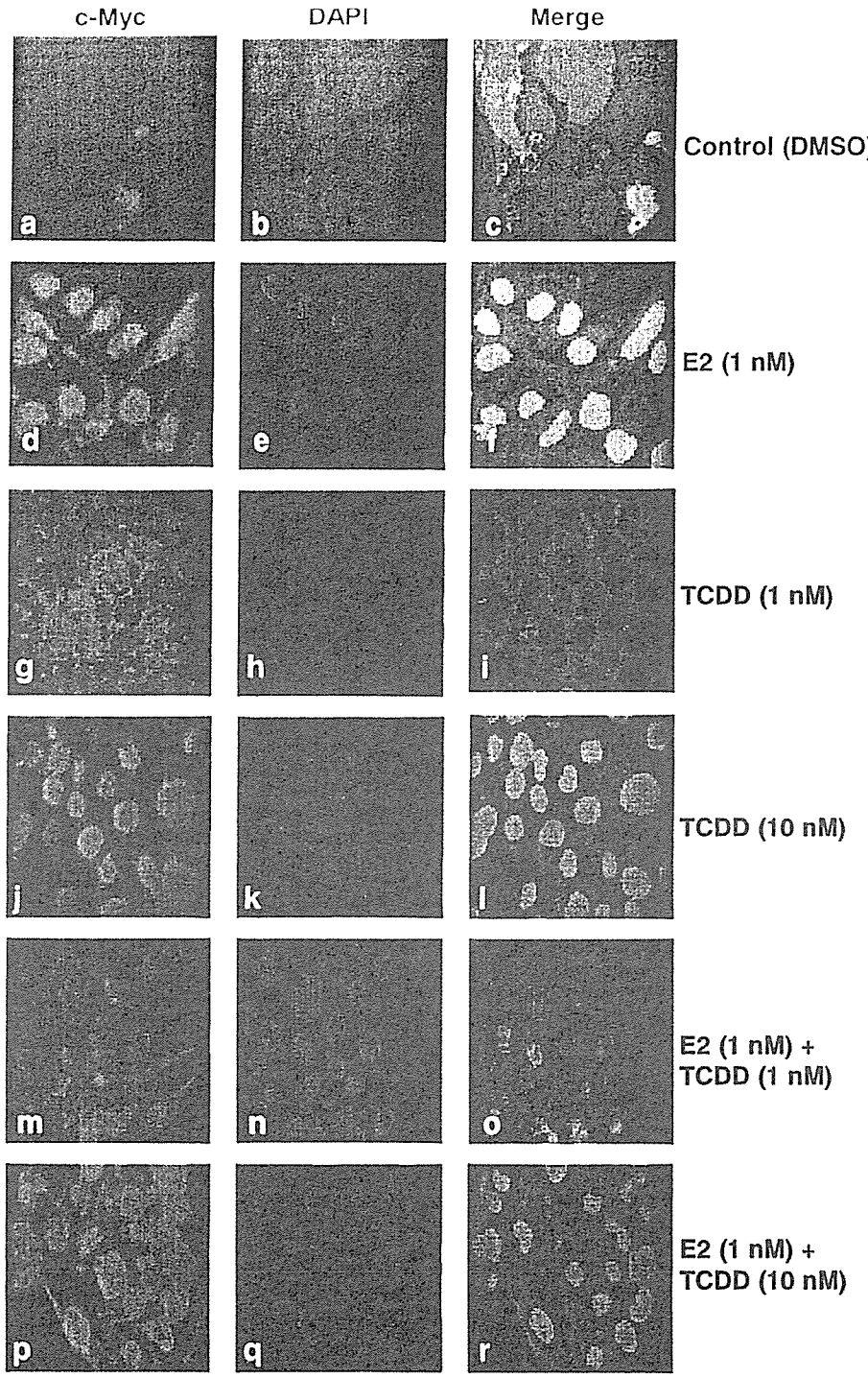

Fig. 5. Immunostaining of c-Myc in BeWo cells. Cells were grown on glass coverslips and then treated for 24 h with either E2 or TCDD alone or in combination. The cells were then washed with chilled PBS and fixed in methanol at -20°C for 12 h. This was followed by treatment with 10% normal goat serum and incubation with c-Myc-specific antibodies and, subsequently, a rhodamine-conjugated secondary antibody. The cells were washed with PBS and stained with 4, 6-2-phenylindole (DAPI). c-Myc protein is visualized by red staining localized in the nucleus while the blue staining indicates nuclear DNA. Merged images confirm the localization of c-Myc in the nucleus.

following 10-nM TCDD treatment, but no activity was induced in these cells by E2 treatment (Fig. 7, right panel). The failure of E2 to induce telomerase in these cell lines can be accounted for by the absence of ER, which further strengthens the hypothesis that functional ER is a requirement for telomerase activation by E2. As expected, TCDD induced telomerase activity in TGR-1 cells but not HO15.19 cells, suggesting that the activation of telomerase by TCDD is directly involved in c-Myc signaling and is different to the mechanisms of *CYP1A1* gene induction.

Discussion

The diverse effects of exposure to TCDD on various biological systems include endocrine disruption, steroid hormone metabolism, interference with cell proliferation and cancer. These

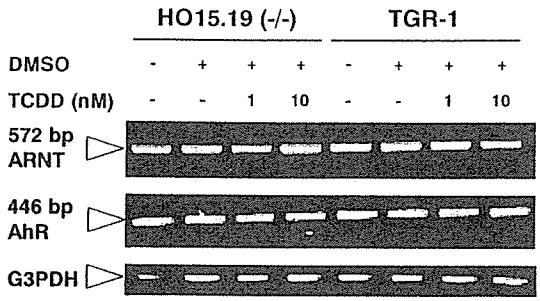

Figure 6. Expression levels of aryl hydrocarbon receptor (AhR) and aryl hydrocarbon nuclear transporter protein (ARNT). HO15.19 and TGR-1 cells were treated with either 1- or 10-nM of TCDD for 24 h prior to RNA isolation. RT-PCR was performed using primers as described in Materials and methods and PCR products were resolved in 1.5% agarose gels and stained with ethidium bromide. G3PDH was used as an internal control.

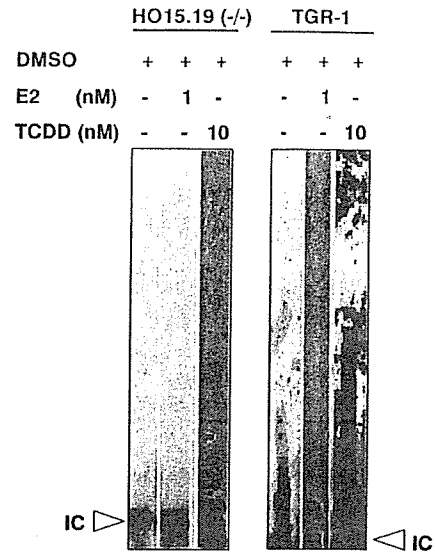

Figure 7. Activation of telomerase by E2 and TCDD in rat fibroblast HO15.19 and TGR-1 cells. Cells were treated with either E2, TCDD or a combination of the two for 24 h and telomerase activity was measured as described in Fig. 1.

effects are mediated by the AhR-ARNT-TCDD complex, either by disruption of signaling cascades or through transcriptional activation of genes containing XRE elements located in upstream promoter regions. TCDD has been established as a potent tumor promoter and has been reviewed extensively (3). Telomerase is involved in cellular immortalization, a type of cell division leading to uncontrolled cell proliferation (25). In the present study we have attempted to address the effects of TCDD on telomerase activity, in order to further understand its role in tumorigenesis.

In BeWo cells, the increase in telomerase activity following 24 h of exposure to TCDD was dose dependent while, no such dose-dependent induction was seen under similar conditions with E2 (Fig. 1). Co-treatment of TCDD with E2 resulted in a marginal decrease in telomerase activity when compared to TCDD treatment alone, which may indicate that TCDD plays a role as a partial agonist that stimulated telomerase activity via ER under the condition of estrogen-unexposed cells and inhibited it in estrogen-treated cells. Such an antagonistic activity of TCDD towards E2 has been reported previously (37). Human telomerase is primarily controlled via its catalytic subunit, hTERT, which is a positive regulator of activity. It is possible, therefore, that TCDD increases hTERT expression levels in a dose-dependent manner, concomitant with elevated telomerase activity. E2 had been shown previously to increase hTERT activity through transcriptional activation of the hTERT promoter by the binding of ER to an ERE (19). However, co-treatment of TCDD and E2 did not result in any cumulative effects on hTERT activity that correlated with the activity of telomerase, as demonstrated in Fig. 1.

Since it has been observed that an increase in telomerase activity was associated with enhanced cell proliferation, the cell proliferation following E2 or TCDD treatment was monitored in the BeWo cells. The results showed that the percentage of the cell population in S-phase was increased by both reagents and that these increases correlated with the telomerase activity induced by the reagents. These findings strongly suggest that TCDD upregulates telomerase, with a concomitant increase in the proliferative index.

Among mitotic signals, c-Myc has been shown to be potentially involved in inducing cell division. In addition, it is well known that E2 can induce c-Myc through transcriptional activation (38) and also that c-Myc is an activator of telomerase (27,39). We therefore analyzed c-Myc induction by both E2 and TCDD treatment and, as shown by Western blotting, a significant increase in c-Myc protein levels was indeed induced by E2 and TCDD (Fig. 4). To confirm this induction of c-Myc protein levels, immunostaining analyses revealed intense nuclear c-Myc staining following either E2 or TCDD treatment (Fig. 5). E2 induction of c-Myc occurs via ER binding to the ERE present upstream of the promoter and this upregulation by both E2 and TCDD may well account for the significant induction of telomerase by both reagents and the increased proliferation of BeWo cells. However, since many other mitogenic signals may also be induced by both E2 and TCDD, which results in activation of telomerase, it was necessary to elucidate further the role of c-Myc in the induction of telomerase by TCDD.

HO15.19 cells (Myc-/-) were used to confirm the involvement of c-Myc-induced telomerase activity via E2 and TCDD. The parental TGR-1 cells, but not the HO15.19 cells, showed induction of telomerase activity by 10-nM TCDD. In addition, HO15.19 cells also failed to show any increase in proliferation following TCDD treatment (data not shown). These findings suggest that c-Myc is involved in the activation of telomerase by TCDD. To our knowledge, this is the first report showing the induction of telomerase by TCDD and the involvement of c-Myc in its induction in BeWo cells. The activation of c-Myc by TCDD might occur directly mediated through transactivation by the AhR-TCDD complex or may occur indirectly via the upregulation of another transcription factor which in turn upregulates c-Myc. In previous studies, it has been suggested that the upstream region of the c-Myc promoter contains a consensus XRE site but functional activity has not been shown (40). The activation of c-Myc by TCDD might occur directly via transcriptional activity or indirectly through the activation of regulatory proteins that enhance transcription. We have analyzed the genome database and determined that the human c-Myc gene does indeed contain consensus XRE elements located at -59, -373, -488 and

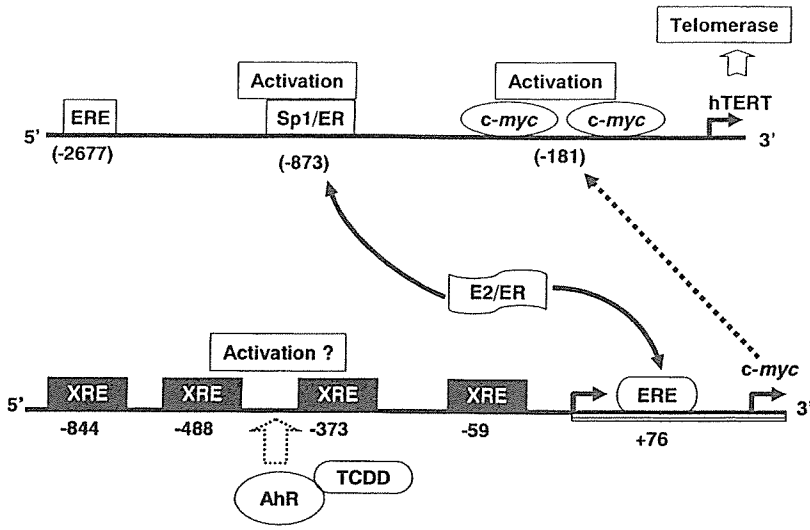

Figure 8. Schematic representation of a possible mechanism for TCDD-induced telomerase activity in BeWo cells. The sequence Accession number for the *c-Myc* gene is M16261 and the hTERT gene structure is adapted from Kyo *et al* (19). The sequence positions are not to scale. Solid arrows indicate binding of E2/ER complexes to their respective cognate sequences in the hTERT and *c-Myc* genes. The dotted arrow indicates a possible mechanism for *c-Myc* binding to the -181 bp sequence present within the core promotor of the hTERT gene. Four putative XRE elements have been identified for TCDD/AhR/ARNT binding but have yet to be characterized. XRE, xenobiotic response element; ERE, estrogen response element.

-884 bp, but it has not yet been established whether these sites are activated by TCDD/AhR/ARNT complexes. While our present study provides strong evidence for the activation of c-Myc by TCDD and the subsequent induction of telomerase activity in BeWo cells, further experiments are needed to validate whether direct transcriptional activation of c-Myc occurs via TCDD.

A possible mechanism for the activation of telomerase by TCDD is represented in the form of a schematic diagram in Fig. 8. As described earlier, E2/ER complexes bind to EREs (-2677 bp) present upstream of the hTERT promoter sequences and activate telomerase. Also present in the hTERT promoter are two c-Myc binding sites within the core promoter (-181 bp) by which c-Myc can directly activate the transcription of hTERT and, subsequently, the telomerase enzyme. In the c-Myc gene regulatory region, there is a half ERE site located at 76 to 80 bp in exon 1 and this may act as an enhancer for activation of the gene by the E2/ER complex. In addition, the c-Myc gene also contains four XRE sites at -59, -373, -488 and -884 bp upstream of the transcription start site and these regions are the most likely binding sites for the TCDD/AhR/ARNT transcriptional complex. The results from the present study indeed suggest that TCDD might activate c-Myc by binding to these XRE sites. c-Myc, in turn, can transactivate the hTERT gene by binding to the -181-bp c-Myc binding site located within the core promoter region. As previously discussed, hTERT is the principal positive regulator of telomerase activity. We could not demonstrate any additive effects of E2 and TCDD upon telomerase activity, indicating that this might be due to the ERE pair present in the c-Myc gene region. Binding of activated ER may, therefore, suppress gene activation by TCDD/AHR/ARNT complexes bound to the more distal ERE site. In TGR-1 cells, which do not express ER, TCDD/AhR/ARNT complexes could activate telomerase, possibly through the activation of c-Myc, further suggesting that the E2/ER complex may hinder the induction of c-Myc in HO15.19 cells.

In conclusion, to our knowledge, this is the first report showing the activation of telomerase by TCDD in BeWo cells. This increase in telomerase activity by TCDD involves the induction of c-Myc, which is the positive regulator of hTERT, and may account for the tumor promoting activity. The present study provides insight into the disruption of telomerase activity and hTERT expression of TCDD.

Acknowledgements

We would like to thank Drs C. Tohyama (Tokyo University, Japan) and S. Sarkar (University of Alabama at Birmingham) for critically reviewing this manuscript. We would like to gratefully acknowledge the Science and Technology Agency (STA) for their financial assistance. PYS is a recipient of an STA fellowship.

References

1. Yonemoto J: The effects of dioxin on reproduction and development. Ind Health 38: 259-268, 2000.
2. Moriguchi T, Motohashi H, Hosoya T, Nakajima O, Takahashi S, Ohsako S, Aoki Y, Nishimura N, Tohyama C, Fujii-Kuriyama Y and Yamamoto M: Distinct response to dioxin in an arylhydrocarbon receptor (AHR)-humanized mouse. Proc Natl Acad Sci USA 100: 5652-5657, 2003.
3. IARC: Monograph on the evaluation of carcinogenic risk to humans: polychlorinated dibenzo-para-dioxins and polychlorinated dibenzofurans. IARC press, Geneva, pp Pages, 1997.
4. Ishimura R, Ohsako S, Kawakami T, Sakaue M, Aoki Y and Tohyama C: Altered protein profile and possible hypoxia in the placenta of 2,3,7,8-tetrachlorodibenzo-*p*-dioxin-exposed rats. Toxicol Appl Pharmacol 185: 197-206, 2002.
5. Davis BJ, McCurdy EA, Miller BD, Lucier GW and Tritscher AM: Ovarian tumors in rats induced by chronic 2,3,7,8-tetrachlorodibenzo-p-dioxin treatment. Cancer Res 60: 5414-5419, 2000.
6. Moran FM, VandeVoort CA, Overstreet JW, Lasley BL and Conley AJ: Molecular target of endocrine disruption in human luteinizing granulosa cells by 2,3,7,8-tetrachlorodibenzo-*p*-dioxin: inhibition of estradiol secretion due to decreased 17alpha-hydroxylase/17,20-lyase cytochrome P450 expression. Endocrinology 144: 467-473, 2003.

7. Safe S: Molecular biology of the Ah receptor and its role in carcinogenesis. Toxicol Lett 120: 1-7, 2001.
8. Whitlock JP Jr: Genetic and molecular aspects of 2,3,7,8-tetrachlorodibenzo-*p*-dioxin action. Annu Rev Pharmacol Toxicol 30: 251-277, 1990.
9. Swanson HI and Bradfield CA: The AH-receptor: Genetics, structure and function. Pharmacogenetics 3: 213-230, 1993.
10. Nebert DW and Jones JE: Regulation of the mammalian cytochrome P1-450 (CYP1A1) gene. Int J Biochem 21: 243-252, 1989.
11. Safe SH: Polychlorinated biphenyls (PCBs): Environmental impact, biochemical and toxic responses, and implications for risk assessment. Crit Rev Toxicol 24: 87-149, 1994.
12. Birnbaum LS: Workshop on perinatal exposure to dioxin-like compounds. V. Immunologic effects. Environ Health Perspect 103 (suppl 2): 157-160, 1995.
13. Jana NR, Sarkar S, Ishizuka M, Yonemoto J, Tohyama C and Sone H: Role of estradiol receptor-alpha in differential expression of 2,3,7,8-tetrachlorodibenzo-*p*-dioxin-inducible genes in the RL95-2 and KLE human endometrial cancer cell lines. Arch Biochem Biophys 368: 31-39, 1999.
14. Thomsen JS, Wang X, Hines RN and Safe S: Restoration of aryl hydrocarbon (Ah) responsiveness in MDA-MB-231 human breast cancer cells by transient expression of the estrogen receptor. Carcinogenesis 15: 933-937, 1994.
15. Wang WL, Thomsen JS, Porter W, Moore M and Safe S: Effect of transient expression of the oestrogen receptor on constitutive and inducible CYP1A1 in Hs578T human breast cancer cells. Br J Cancer 73: 316-322, 1996.
16. Sarkar S, Jana NR, Yonemoto J, Tohyama C and Sone H: Estrogen enhances induction of cytochrome P-4501A1 by 2,3,7, 8-tetrachlorodibenzo-*p*-dioxin in liver of female Long-Evans rats. Int J Oncol 16: 141-147, 2000.
17. Ohtake F, Takeyama K, Matsumoto T, Kitagawa H, Yamamoto Y, Nohara K, Tohyama C, Krust A, Mimura J, Chambon P, Yanagisawa J, Fujii-Kuriyama Y and Kato S: Modulation of oestrogen receptor signalling by association with the activated dioxin receptor. Nature 423: 545-550, 2003.
18. Chaffin CL, Peterson RE and Hutz RJ: *In utero* and lactational exposure of female Holtzman rats to 2,3,7,8-tetrachlorodibenzo-*p*-dioxin: Modulation of the estrogen signal. Biol Reprod 55: 62-67, 1996.
19. Kyo S, Takakura M, Kanaya T, Zhuo W, Fujimoto K, Nishio Y, Orimo A and Inoue M: Estrogen activates telomerase. Cancer Res 59: 5917-5921, 1999.
20. Greider CW and Blackburn EH: A telomeric sequence in the RNA of Tetrahymena telomerase required for telomere repeat synthesis. Nature 337: 331-337, 1989.
21. Blackburn EH: Telomerases. Annu Rev Biochem 61: 113-129, 1992.
22. Hayflick L and Moorhead PS: The serial cultivation of human diploid cell strains. Exp Cell Res 25: 585-621, 1961.
23. Harley CB, Futcher AB and Greider CW: Telomeres shorten during ageing of human fibroblasts. Nature 345: 458-460, 1990.
24. Avilion AA, Piatyszek MA, Gupta J, Shay JW, Bacchetti S and Greider CW: Human telomerase RNA and telomerase activity in immortal cell lines and tumor tissues. Cancer Res 56: 645-650, 1996.
25. Greider CW: Telomere length regulation. Annu Rev Biochem 65: 337-365, 1996.
26. Shay JW and Bacchetti S: A survey of telomerase activity in human cancer. Eur J Cancer 33: 787-791, 1997.
27. Wu KJ, Grandori C, Amacker M, Simon-Vermot N, Polack A, Lingner J and Dalla-Favera R: Direct activation of TERT transcription by c-MYC. Nat Genet 21: 220-224, 1999.
28. Rea MA, Phillips MA, Degraffenried LA, Qin Q and Rice RH: Modulation of human epidermal cell response to 2,3,7,8-tetrachlorodibenzo-*p*-dioxin by epidermal growth factor. Carcinogenesis 19: 479-483, 1998.
29. Jiang SW, Lloyd RV, Jin L and Eberhardt NL: Estrogen receptor expression and growth-promoting function in human choriocarcinoma cells. DNA Cell Biol 16: 969-977, 1997.
30. Lewintre EJ, Orava M and Vihko R: Regulation of 17 beta-hydroxysteroid dehydrogenase type 1 by epidermal growth factor and transforming growth factor-alpha in choriocarcinoma cells. Endocrinology 135: 2629-2634, 1994.
31. Tatematsu K, Nakayama J, Danbara M, Shionoya S, Sato H, Omine M and Ishikawa F: A novel quantitative 'stretch PCR assay', that detects a dramatic increase in telomerase activity during the progression of myeloid leukemias. Oncogene 13: 2265-2274, 1996.
32. Bieche I, Nogues C, Paradis V, Olivi M, Bedossa P, Lidereau R and Vidaud M: Quantitation of hTERT gene expression in sporadic breast tumors with a real-time reverse transcription-polymerase chain reaction assay. Clin Cancer Res 6: 452-459, 2000.
33. Nakamura TM, Morin GB, Chapman KB, Weinrich SL, Andrews WH, Lingner J, Harley CB and Cech TR: Telomerase catalytic subunit homologs from fission yeast and human. Science 277: 955-959, 1997.
34. Nugent CI and Lundblad V: The telomerase reverse transcriptase: components and regulation. Genes Dev 12: 1073-1085, 1998.
35. Ben-Yosef T, Yanuka O, Halle D and Benvenisty N: Involvement of Myc targets in c-myc and N-myc induced human tumors. Oncogene 17: 165-171, 1998.
36. Mateyak MK, Obaya AJ, Adachi S and Sedivy JM: Phenotypes of c-Myc-deficient rat fibroblasts isolated by targeted homologous recombination. Cell Growth Differ 8: 1039-1048, 1997.
37. Cheng J and Malayer JR: Responses to stable ectopic estrogen receptor-beta expression in a rat fibroblast cell line. Mol Cell Endocrinol 156: 95-105, 1999.
38. Porter W, Wang F, Duan R, Qin C, Castro-Rivera E, Kim K and Safe S: Transcriptional activation of heat shock protein 27 gene expression by 17beta-estradiol and modulation by antiestrogens and aryl hydrocarbon receptor agonists. J Mol Endocrinol 26: 31-42, 2001.
39. Shiu RP, Watson PH and Dubik D: c-myc oncogene expression in estrogen-dependent and -independent breast cancer. Clin Chem 39: 353-355, 1993.
40. Wang J, Xie LY, Allan S, Beach D and Hannon GJ: Myc activates telomerase. Genes Dev 12: 1769-1774, 1998.
41. Kim DW, Gazourian L, Quadri SA, Romieu-Mourez R, Sherr DH and Sonenshein GE: The RelA NF-kappaB subunit and the aryl hydrocarbon receptor (AhR) cooperate to transactivate the c-myc promoter in mammary cells. Oncogene 19: 5498-5506, 2000.

0888-8809/06/$15.00/0
Printed in U.S.A.

Molecular Endocrinology 20(9):2141–2155

doi: 10.1210/me.2005-0367

Endocrine-Disrupting Organotin Compounds Are Potent Inducers of Adipogenesis in Vertebrates

Felix Grün, Hajime Watanabe, Zamaneh Zamanian, Lauren Maeda, Kayo Arima, Ryan Cubacha, David M. Gardiner, Jun Kanno, Taisen Iguchi, and Bruce Blumberg

Department of Developmental and Cell Biology (F.G., Z.Z., L.M., K.A., R.C., D.M.G., B.B.), University of California Irvine, Irvine California 92697-2300; National Institutes of Natural Sciences (H.W., T.I.), National Institute for Basic Biology, Okazaki Institute for Integrative Bioscience, Okazaki 444-8787, Japan; and Division of Cellular & Molecular Toxicology (J.K.), Biological Safety Research Center, National Institute of Health Sciences, Setagaya-ku, Tokyo 158-8501, Japan

Dietary and xenobiotic compounds can disrupt endocrine signaling, particularly of steroid receptors and sexual differentiation. Evidence is also mounting that implicates environmental agents in the growing epidemic of obesity. Despite a long-standing interest in such compounds, their identity has remained elusive. Here we show that the persistent and ubiquitous environmental contaminant, tributyltin chloride (TBT), induces the differentiation of adipocytes *in vitro* and increases adipose mass *in vivo*. TBT is a dual, nanomolar affinity ligand for both the retinoid X receptor (RXR) and the peroxisome proliferator-activated receptor γ (PPARγ). TBT promotes adipogenesis in the murine 3T3-L1 cell model and perturbs key regulators of adipogenesis and lipogenic pathways *in vivo*. Moreover, *in utero* exposure to TBT leads to strikingly elevated lipid accumulation in adipose depots, liver, and testis of neonate mice and results in increased epididymal adipose mass in adults. In the amphibian *Xenopus laevis*, ectopic adipocytes form in and around gonadal tissues after organotin, RXR, or PPARγ ligand exposure. TBT represents, to our knowledge, the first example of an environmental endocrine disrupter that promotes adipogenesis through RXR and PPARγ activation. Developmental or chronic lifetime exposure to organotins may therefore act as a chemical stressor for obesity and related disorders. (*Molecular Endocrinology* 20: 2141–2155, 2006)

ORGANOTINS ARE A diverse group of widely distributed environmental pollutants. Tributyltin chloride (TBT) and bis(triphenyltin) oxide (TPTO), have pleiotropic adverse effects on both invertebrate and vertebrate endocrine systems. Organotins were first used in the 1960s as antifouling agents in marine shipping paints, although such use has been restricted in recent years. Organotins persist as prevalent contaminants in dietary sources, such as fish and shellfish, and through pesticide use on high-value food crops (1, 2). Additional human exposure to organotins may occur through their use as antifungal agents in wood treatments, industrial water systems, and textiles. Mono- and diorganotins are prevalently used as stabilizers in the manufacture of polyolefin plastics (polyvinyl chloride), which introduces the potential for transfer by contact with drinking water and foods.

Exposure to organotins such as TBT and TPTO results in imposex, the abnormal induction of male sex characteristics in female gastropod mollusks (3, 4). Bioaccumulation of organotins decreases aromatase activity leading to a rise in testosterone levels that promotes development of male characteristics (5). Imposex results in impaired reproductive fitness or sterility in the affected animals and is one of the clearest examples of environmental endocrine disruption. TBT exposure also leads to masculinization of at least two fish species (6, 7), but TBT is only reported to have modest adverse effects on mammalian male and female reproductive tracts and does not alter sex ratios (8, 9). Instead, hepatic-, neuro-, and immunotoxicity appear to be the predominant effects of organotin exposure (10). Hence, the current mechanistic understanding of the endocrine-disrupting potential of organotins is based on their direct actions on the levels or activity of key steroid-regulatory enzymes such as aromatase and more general toxicity mediated via damage to mitochondrial functions and subsequent cellular stress responses (11–15).

However, it remains an open question whether *in vivo* organotins act primarily as protein and enzyme

First Published Online April 13, 2006

Abbreviations: Acac, Acetyl-coenzyme A carboxylase; b.w., body weight; C/EBP, CCAAT/enhancer binding protein; 9-*cis* RA, 9-cis retinoic acid; DMSO, dimethylsulfoxide; F, forward; Fatp, fatty acid transport protein; LBD, ligand-binding domain; LXR, liver X receptor; MDIT, 3-isobutyl-1-methylxanthine, dexamethasone, insulin and T_3 adipocyte differentiation mix; PPAR, peroxisome proliferator-activated receptor; R, reverse; RAR, retinoic acid receptor; RXR, retinoid X receptor; Srebf1, sterol-regulatory element binding factor 1; TBT, tributyltin chloride; TPTO, triphenyltin oxide; TTNPB, (E)-4-[2-(5,6,7,8-tetrahydro-5,5,8,8-tetramethyl-2-naphthylenyl)-1-propenyl] benzoic acid; VDR, vitamin D receptor.

***Molecular Endocrinology* is published monthly by The Endocrine Society (http://www.endo-society.org), the foremost professional society serving the endocrine community.**

inhibitors, or rather mediate their endocrine-disrupting effects at the transcriptional level. Recent work has shown that aromatase mRNA levels can be down-regulated in human ovarian granulosa cells by treatment with organotins or ligands for the nuclear hormone receptors, retinoid X receptor (RXRs) or peroxisome proliferator-activated receptor γ (PPARγ) (16–18). Furthermore, Nishikawa *et al.* (19) have demonstrated that the gastropod *Thais clavigara* RXR homolog is responsive to 9-cis-retinoic acid (9-*cis*-RA) and TBT, and 9-*cis* RA can also induce imposex, suggesting a conserved transcriptional mechanism for TBT action across phyla. These ligand-dependent transcription factors belong to the nuclear hormone receptor superfamily—a group of approximately 150 members (48 human genes) that includes the estrogen receptor, androgen receptor, glucocorticoid receptor, thyroid hormone receptor, vitamin D receptor (VDR), retinoic acid receptors (RARs and RXRs), PPARs, and numerous orphan receptors. We were therefore intrigued by the similar effects of TBT and RXR/PPARγ ligands on mammalian aromatase mRNA expression and hypothesized that TBT might be exerting some of its biological effects via transcriptional regulation of gene expression through activation of one or more nuclear hormone receptors.

Our results show that organotins such as TBT are indeed potent and efficacious agonistic ligands of the vertebrate nuclear receptors, retinoid X receptors (RXRs) and PPARγ. The physiological consequences of receptor activation predict that permissive RXR heterodimer target genes and downstream signaling cascades are sensitive to organotin misregulation. Consistent with this prediction we observe that organotins phenocopy the effects of RXR and PPARγ ligands using *in vitro* and *in vivo* models of adipogenesis. Therefore, TBT and related organotin compounds are the first of a potentially new class of environmental endocrine disrupters that targets adipogenesis by modulating the activity of key regulatory transcription factors in the adipogenic pathway, RXRα and PPARγ. The existence of such xenobiotic compounds was previously hypothesized (20, 21). Our results suggest that developmental exposure to TBT and its congeners that activate RXR/PPARγ might be expected to increase the incidence of obesity in exposed individuals and that chronic lifetime exposure could act as a potential chemical stressor for obesity and obesity-related disorders.

RESULTS

Organotins Are Agonists of Vertebrate RXR and RXR-Permissive Heterodimers

Many known or suspected environmental endocrine-disrupting chemicals mimic natural lipophilic hormones that act through members of the superfamily of nuclear receptor transcription factors (22, 23). In a screen of high-priority endocrine-disrupting chemicals against a bank of vertebrate nuclear receptor ligand-binding domains (LBDs), we observed that organotins, specifically tributyltin chloride (TBT) and bis(triphenyltin) oxide (TPTO), could fully activate an RXRα LBD construct (GAL4-RXRα) in transient transfection assays. Both TBT and TPTO were as potent (EC_{50} ~3–10 nM) as 9-*cis* retinoic acid, an endogenous RXR ligand and approximately 2- to 5-fold less potent than the synthetic RXR-specific ligands LG100268 (EC_{50} ~ 2 nM) or AGN195203 (EC_{50} ~ 0.5 nM) (Fig. 1A and see Table 2). Maximal activation for TBT reached the same levels as LG100268 or AGN195203.

We next tested whether activation by TBT was unique to RXRα only, restricted to RXR heterodimer complexes, or a general nuclear receptor transcriptional response (Fig. 1, B–D, and Table 1). TBT activated RXRα and RXRγ from the amphibian *Xenopus laevis* in addition to human RXRs (Table 1). Our results are consistent with recent findings by Nishikawa *et al.* (19, 24) that organotins promote activation of all three human RXR subtypes in a yeast two-hybrid screen. We also observed significant activation of receptors typically considered to be permissive heterodimeric partners of RXR including human PPARγ (Fig. 1B, ~30% maximal activation of 10 μM troglitazone, but note that activation is compromised by cellular toxicity above 100 nM), PPARδ, liver X receptor (LXR), and the orphan receptor NURR1. In contrast, typical nonpermissive partners such as RARs, thyroid hormone receptor, and VDR failed to show activation by organotins (Fig. 1C and Table 1). Murine PPARα was also not activated by TBT although it was fully activated by its specific synthetic agonist WY-14643 (Fig. 1D). The steroid and xenobiotic receptor was likewise unresponsive. The orphan receptor NURR1, which has no discernable ligand pocket and is believed to be ligand independent (25), was nevertheless activated 7- to 10-fold at 100 nM TBT. Similarly, other RXR-specific ligands, *e.g.* LG100268, activated NURR1 to the same degree, suggesting that this response occurred through NURR1's heterodimeric partner RXR as has been previously described (25, 26). Like other RXR-specific ligands, tributyltin was also able to promote the ligand-dependent recruitment of nuclear receptor cofactors such as receptor-associated coactivator 3 (ACTR), steroid receptor coactivator-1, and PPAR-binding protein in mammalian two-hybrid interaction assays (data not shown). We infer from these results that nuclear receptor activation by TBT activation is specific to a small subset of receptors and not a consequence of a general effect on the cellular transcriptional machinery.

We next investigated the relationship between the structure of the tin compounds and RXR activation by testing the response of GAL4-RXRα to mono-, di-, tri-, and tetra-substituted butyltin, branched side chains, variations in the alkyl chain length, and changes in the halide component (Fig. 1A and Table 2). Overall, trialkyltin compounds were the most effective with nano-

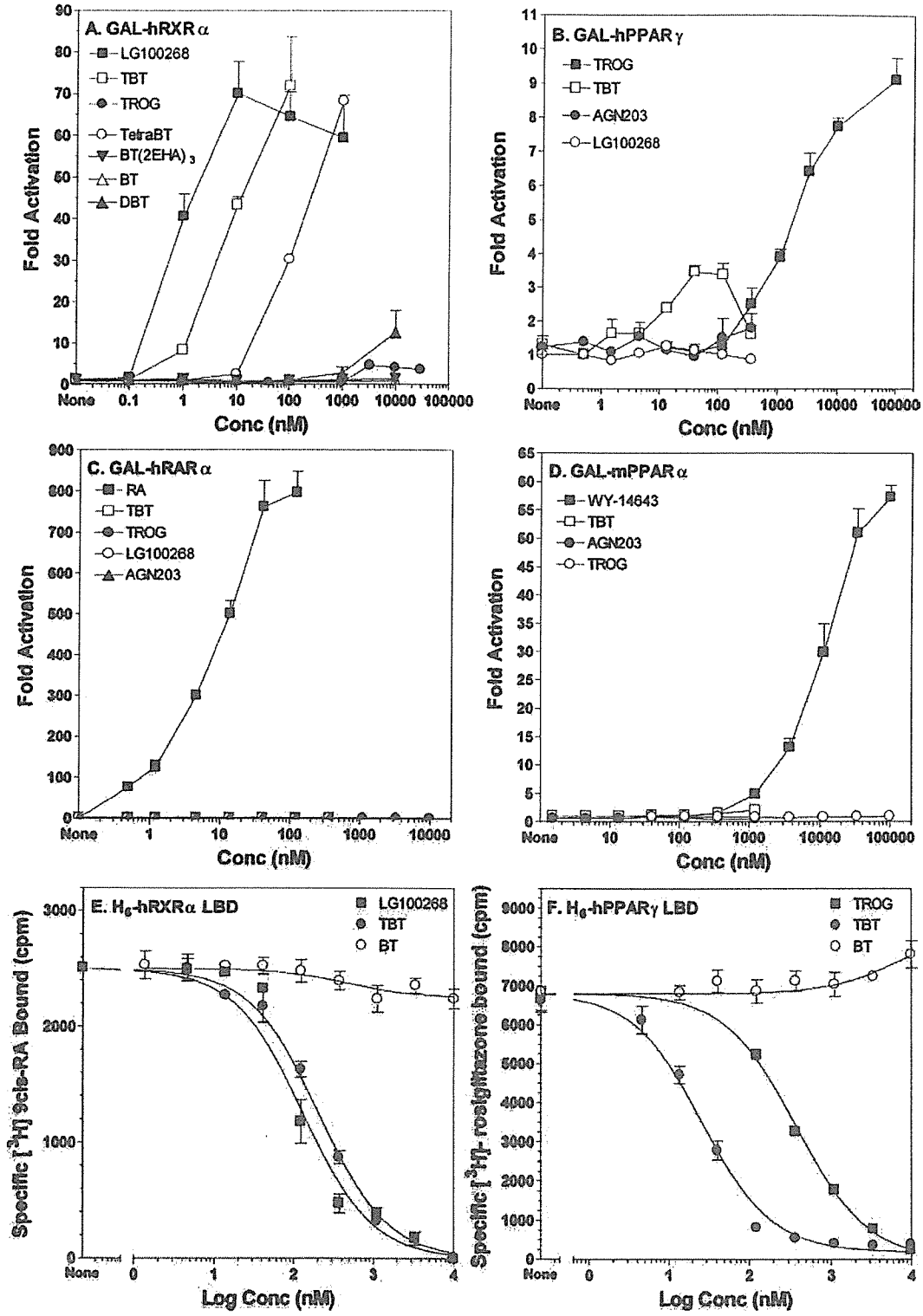

Fig. 1. Organotins Are Agonist Ligands of RXRα and PPARγ

Organotins are high-affinity ligand agonists of RXRα and PPARγ. A–D, Activation of GAL4-hRXRα, -hPPARγ, -hRARα, or -hPPARα in transiently transfected Cos7 cells by organotins and receptor-specific ligands. Data represent reporter luciferase activity normalized to β-galactosidase and plotted as the average fold activation ± SEM (n = 3) relative to solvent-only controls from representative experiments. E and F, Competition binding curves of histidine-tagged RXRα or PPARγ LBDs with TBT. Data shown are from a representative experiment analyzed in GraphPad Prism 4.0 and K_i values deduced (Table 3). Conc, Concentration; DBT, dibutyltin chloride; TROG, troglitazone.

Table 1. TBT Activates RXRs and RXR-Permissive Heterodimers

GAL4-NR LBD	Fold Activation at 60 nM TBT	Permissive RXR Heterodimer
RXRα (*Homo sapiens*)	60	Yes
RXRα (*X. laevis*)	25	Yes
RXRγ (*X. laevis*)	7.0	Yes
NURR1 (*H. sapiens*)	7.0	Yes
LXR (*H. sapiens*)	2.1	Yes
PPARα (*Mus musculus*)	0.7	Yes
PPARγ (*H. sapiens*)	5.3	Yes
PPARδ (*H. sapiens*)	1.7	Yes
RARα (*H. sapiens*)	0.7	No
TR&β (*H. sapiens*)	0.4	No
VDR (*H. sapiens*)	0.5	No
SXR (*H. sapiens*)	1.0	No

Data are fold activation at 60 nM TBT relative to solvent-only controls of transiently transfected Cos7 cells after 24 h ligand treatment. SXR, Steroid and xenobiotic receptor; TR, thyroid hormone receptor.

molar EC_{50} values. Monobutyltin gave no significant activation whereas dibutyltin was moderately active in the micromolar range (Fig. 1A and Table 2). Tetrabutyltin was 20-fold less potent than TBT, whereas the branched side-chain butyltin tris(2-ethylhexanoate) [BT(2-EHA)$_3$] was inactive (Table 2). Although activation by dialkyltins is weaker than that of TBT, it is potentially significant due to their widespread use in the manufacture of polyvinyl chloride plastics and greater solubility than TBT.

The effect of the hydrocarbon chain length was very pronounced, suggesting an important structure-activity relationship. A reduction in hydrophobicity from butyl to ethyl side chains raised the EC_{50} value by almost 1000-fold into the micromolar range. Trimethyltin was weakly active only above 100 μM (Table 2). Substitution of the halide component had no significant effect on the EC_{50} values for TBT, probably due to the lability of the halide atom through exchange in aqueous tissue culture media where chloride ions are prevalent.

Table 2. Organotin EC_{50} Values for Nuclear Receptor LBDs

Ligand	GAL4-NR LBD Transactivation (EC_{50} Values, nM)		
	hRXRα	hRARα	hPPARγ
LGD268	2–5	na	na
AGN195203	0.5–2	na	na
9-*cis* RA	15	na	na
all-*trans* RA	na	8	na
Butyltin chloride	na	na	na
Dibutyltin chloride	3000	na	na
TBT	3–8	na	20
Tetrabutyltin	150	ND	ND
Di(triphenyltin)oxide	2–10	na	20
Butyltin tris(2-ethylhexanoate)	na	ND	ND
Troglitazone	na	na	1000
Tributyltin fluoride	3	ND	ND
Tributyltin bromide	4	ND	ND
Tributyltin iodide	4	ND	ND
Triethyltin bromide	2800	ND	ND
Trimethyltin chloride	>10000	ND	ND

na, Not active; ND, not determined. EC_{50} values were determined from dose-response curves of GAL4-NR LBD construct activation in transiently transfected Cos7 cells after 24-h ligand exposure.

TBT Is a Potent Ligand of Both RXRα and PPARγ

Many, if not most, natural and synthetic nuclear receptor agonists act as ligands that specifically interact with their cognate receptor LBDs. We therefore performed equilibrium competition binding experiments with purified histidine-tagged human RXRα (H_6-RXRα) and PPARγ (H_6-PPARγ) LBDs to determine whether the potent and specific activation of these receptors by TBT was due to direct ligand-receptor interaction (Fig. 1, E and F).

The equilibrium binding curves indicate that TBT is a high-affinity, competitive ligand for 9-*cis* RA-bound RXRα. The inhibition equilibrium dissociation constant was calculated by the Chang-Prusoff method [inhibition constant (K_i) = dissociation constant (K_d)] as 12.5 nM (10–15 nM; 95% confidence interval) (Table 3). By comparison, the value obtained for the synthetic RXR agonist LG100268 was 7.5 nM, which compared favorably with its published value of approximately 3 ± 1 nM (27). Therefore, the identification of TBT as an RXR ligand expands the molecular definition of known rexinoids (agonists able to activate RXR) to include this structurally unique class of organotin compounds.

Somewhat surprisingly, we also observed potent specific competitive binding by TBT for rosiglitazone bound to human PPARγ LBD (Fig. 2B). The deduced K_i of 20 nM (17–40 nM; 95% confidence interval) was slightly higher than for RXRα but significantly better than the K_i for the PPARγ agonist troglitazone, which

Table 3. TBT Binding Constants (K_d) for hRXRα and hPPARγ LBDs

Ligand	Receptor Competitive Inhibition Binding Constants K_i (nM ± 95% CI)		
	H_6-RXRα	H_6-PPARγ	Published
TBT	12.5 (10–15)	20 (17–40)	
LG100268	7.5 (6–10)	ND	3 ± 1[a]
Troglitazone	ND	300 (270–335)	300 ± 30[b]

Competition binding curves were determined at constant ^{3}H-specific ligand concentrations [20 nM 9-*cis*-RA, K_d = 1.4 nM (87) or rosiglitazone, K_d = 41 nM (88)] with increasing cold competitor ligands over the range indicated in Fig. 1, E and F. Data were analyzed in GraphPad Prism by nonlinear regression of a competitive one-site binding equation (Chang-Prusoff method) to determine K_i values ± 95% confidence intervals (n = 3). CI, Confidence interval; ND, not determined.
[a] RXRα:LG100268 K_d = 3 ± 1 nM (27).
[b] PPARγ:troglitazone K_d = 300 ± 30 nM (28).

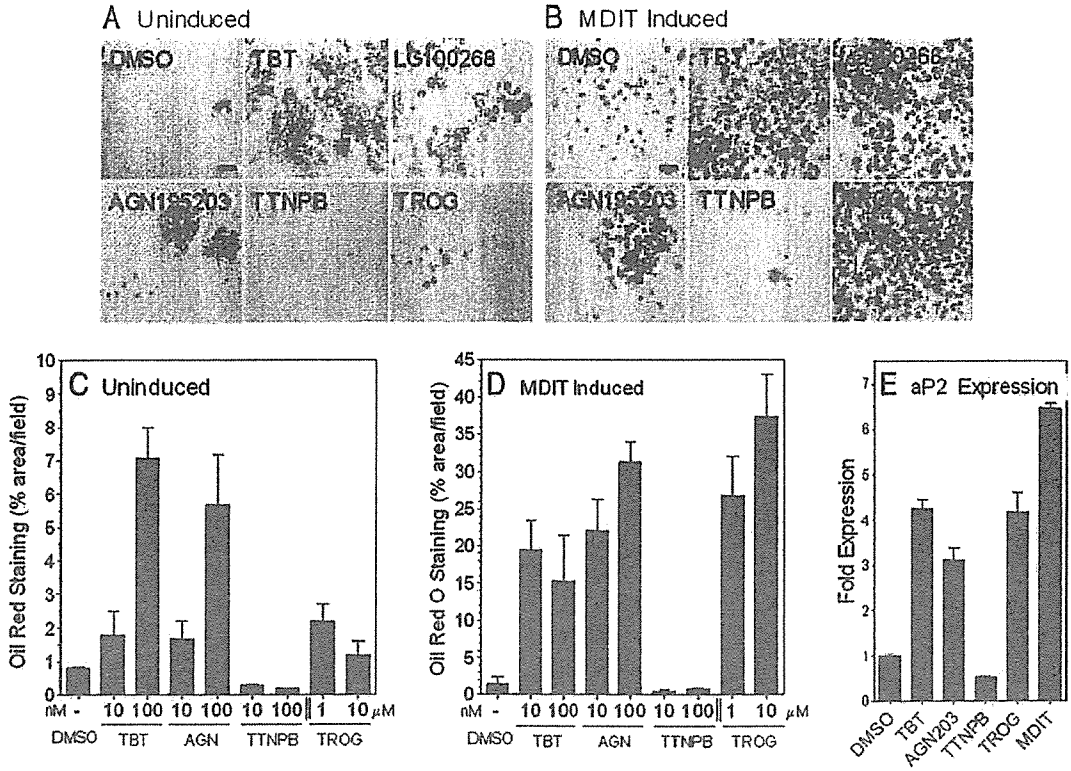

Fig. 2. Tributyltin Induces Adipogenesis in 3T3-L1 Cells

Uninduced (A) and MDIT-induced (B) 3T3-L1 cultures grown for 1 wk in the presence of vehicle (DMSO), or ligands were analyzed for mature adipocyte differentiation by Oil Red O staining. *Scale bar* represents 100 μm. C and D, The percentage area stained was determined by automated analysis of random fields (n = 9) from high-contrast dissecting scope photographs of monolayers analyzed in ImageJ; 1–100 nM of TBT, AGN195203, and TTNPB or 1–10 μM troglitazone. E, Quantitative real-time PCR (QRT-PCR) of adipocyte-specific fatty acid binding protein aP2 (aP2/Fabp4) expression levels in postconfluent 3T3-L1 cells treated with the indicated ligands for 24 h. Data were normalized to glyceraldehyde-3-phosphate dehydrogenase controls and plotted as average fold induction ± SEM (n = 3).TROG, Troglitazone.

yielded a K_i of 300 nM, consistent with its published K_d (28). The K_d values for TBT binding to RXRα (12.5 nM) and PPARγ (20 nM) are also in close agreement with EC_{50} values obtained from transient transfection assays using GAL4-RXRα and GAL4-PPARγ constructs (Table 2).

Taken together, these data show that organotins such as TBT, although structurally distinct from previously described natural or synthetic ligands, can interact with RXRα and PPARγ, via direct ligand binding to induce productive receptor-coactivator interactions and promote transcription in a concentration-dependent manner. Organotins are therefore potent nanomolar receptor activators on par with synthetic RXR and PPARγ ligands such as LG100268, AGN195203, and thiazolidinediones.

TBT Promotes Adipogenesis in the Murine 3T3-L1 Cell (Embryonic Murine Preadipocyte Fibroblast Cell Line) Model

Numerous studies have demonstrated the critical role played by RXRα:PPARγ signaling in regulation of mammalian adipogenesis (29–31). In the murine 3T3-L1 preadipocyte cell model, adipogenic signals induce early key transcriptional regulators such as CCAAT/enhancer binding proteins (C/EBPs) β and δ that lead to mitotic clonal expansion of growth-arrested preadipocytes and induction of the late differentiation factors C/EBPα and PPARγ (32–34). The combination of C/EBPα expression together with PPARγ signaling efficiently drives terminal adipocyte differentiation and lipid accumulation. We therefore tested whether TBT signaling through RXR:PPARγ could promote adipogenesis in the murine 3T3-L1 differentiation assay and compared its effect to other RXR-specific or PPARγ ligands (Fig. 2). Undifferentiated 3T3-L1 cells were cultured for 1 wk in the presence of ligands either with or without a prior 2-d treatment with MDIT (an adipogenic-sensitizing cocktail of 3-isobutyl-1-methylxanthine, dexamethasone, insulin, and T_3) (35). Cells were then scored for lipid accumulation using Oil Red O staining to determine the degree of terminal adipocyte differentiation. TBT was as effective as LG100268 or AGN195203 in promoting dif-

ferentiation in the absence of MDIT treatment, increasing the number of differentiated adipocytes about 7-fold over solvent-only controls (Fig. 2, A and C). The PPARγ agonist troglitazone was a weak inducer in the absence of MDIT. Prior treatment with MDIT increased the response to TBT, LG100268, and AGN195203 a further 3- to 5-fold (Fig. 2, B and D). MDIT treatment also boosted the response to troglitazone to equivalent levels as expected from published studies showing that combination treatment with PPARγ ligands promotes efficient adipocyte differentiation (36–38). In contrast, the RAR agonist TTNPB inhibited the differentiation of 3T3-L1 cells, consistent with previously published data that showed RAR signaling blocks adipogenesis during the early stages of differentiation *in vitro* and can modulate adiposity and whole body weight *in vivo* (39–41). The differential response of 3T3-L1 cells to receptor-selective retinoids indicates that TBT favors RXR homodimer or permissive RXR-heterodimer rather than RXR:RAR signaling in this cell model.

Adipocyte differentiation by TBT was accompanied by direct transcriptional effects on RXR:PPARγ targets such as adipocyte-specific fatty acid-binding protein (aP2) mRNA. The aP2 promoter contains response elements sensitive to C/EBP factors and RXRα:PPARγ signaling (42). Quantitative real-time PCR analysis showed aP2 levels were elevated by TBT treatment approximately 5-fold at 24 h (Fig. 2E) and 45-fold at 72 h (data not shown). LG100268, troglitazone, and MDIT treatment also increased aP2 expression at these time points whereas the RAR agonist TTNPB was inhibitory, consistent with the observed cellular responses.

TBT Induces Adipogenic Regulators and Markers of RXRα:PPARγ Signaling *in Vivo*

The ability of organotins to regulate RXRα:PPARγ target genes and key modulators of adipogenesis and lipid homeostasis *in vivo* has not been previously examined. Therefore, we next asked whether TBT could perturb expression of critical transcriptional mediators of adipogenesis such as RXRα, PPARγ, C/EBPα/β/δ, and sterol regulatory element binding factor 1 (Srebf1) as well as known target genes of RXRα:PPARγ signaling from liver, epididymal adipose tissue, and testis of 6-wk-old male mice dosed for 24 h with TBT [0.3 mg/kg body weight (b.w.)], AGN195203 (0.3 mg/kg b.w.), troglitazone (3 mg/kg b.w), or vehicle (corn oil) administered by ip injection. TBT either had no effect or weakly repressed RXRα and PPARγ transcription in liver (Fig. 3, A and B). A more pronounced decrease was observed for RXRα, PPARγ, C/EBPα, and C/EBPδ in adipose tissue and testis (Fig. 3, B and C). In contrast, TBT, AGN195203, and troglitazone significantly induced expression of the early adipogenic transcription factor C/EBPβ in liver and testis, whereas it was more weakly induced in adipose tissue. Induction was strongest in testis where TBT and troglitazone increased expression greater than 10-fold and AGN195203 increased expression 60-fold compared with vehicle controls (Fig. 3C). In addition to C/EBPβ, the proadipogenic transcription factor Srebf1 was also significantly increased in adipose tissue by all three receptor ligands and weakly induced in liver.

We also observed coordinate changes in several well-characterized direct target genes of RXR:PPARγ signaling. Fatty acid transport protein (Fatp) acts as a key control point for regulation of cellular fatty acid content. The Fatp promoter contains a functional PPAR response element shown to be sensitive to RXR:PPARγ signaling in 3T3-L1 adipocytes and white fat (43–46). Fatp mRNA levels were up regulated 2- to 3-fold in liver and epididymal adipose tissue but not testis by TBT, AGN195203, and troglitazone (see Fig. 5, A and B). Similarly, the PPARγ target phosphoenolpyruvate carboxykinase 1 (PEPCK/Pck1) (47), the rate-limiting step in hepatic gluconeogenesis and adipose glyceroneogenesis, was up-regulated in liver and adipose tissues by TBT or troglitazone treatment.

Signaling through RXR:PPARγ, RXR:LXR, and ADD1/Srebf1 in hepatocytes has been shown to modulate fatty acid synthesis through transcriptional control of acetyl-coenzyme A carboxylase (Acac), the rate-limiting step in long-chain fatty acid synthesis (48, 49), as well as fatty acid synthase (Fasn) (50–53). Hepatic expression of both Acac and Fasn was unregulated between 1.5–2.5-fold by TBT, AGN195203, and troglitazone. Therefore, the coordinate increased expression of Fatp, Pck1, Acac, and Fasn in liver suggests that TBT stimulates fatty acid uptake and triglyceride synthesis. Similar changes have been reported in the induction of hepatic steatosis by overactive PPARγ signaling (49, 54).

Taken together, these data show that TBT exposure induces lipogenic RXR:PPARγ target gene expression, in adipose tissue and liver, and modulates associated early adipocyte differentiation factors such as C/EBPβ and Srebf1. We inferred from these data that organotins are potential adipogenic agents *in vivo*.

Developmental Exposure to TBT Disrupts Lipid Homeostasis and Adipogenesis in Vertebrates

Based on its molecular pharmacology, ability to induce 3T3-L1 adipocyte differentiation, and *in vivo* transcriptional responses, we reasoned that TBT would disrupt normal endocrine control over lipid homeostasis and impact adipogenesis, particularly when exposure occurred during sensitive periods of development. We therefore tested this hypothesis in two vertebrate model systems, mouse and *X. laevis*, during embryogenesis.

Pregnant C57BL/6 mice were injected daily from gestational d 12–18 with TBT (0.05 or 0.5 mg/kg body weight ip) dissolved in sesame oil or vehicle alone. Pups were then killed at birth, and histological sections were prepared from liver, testis, mammary gland, and inguinal adipose tissue. Sections were stained

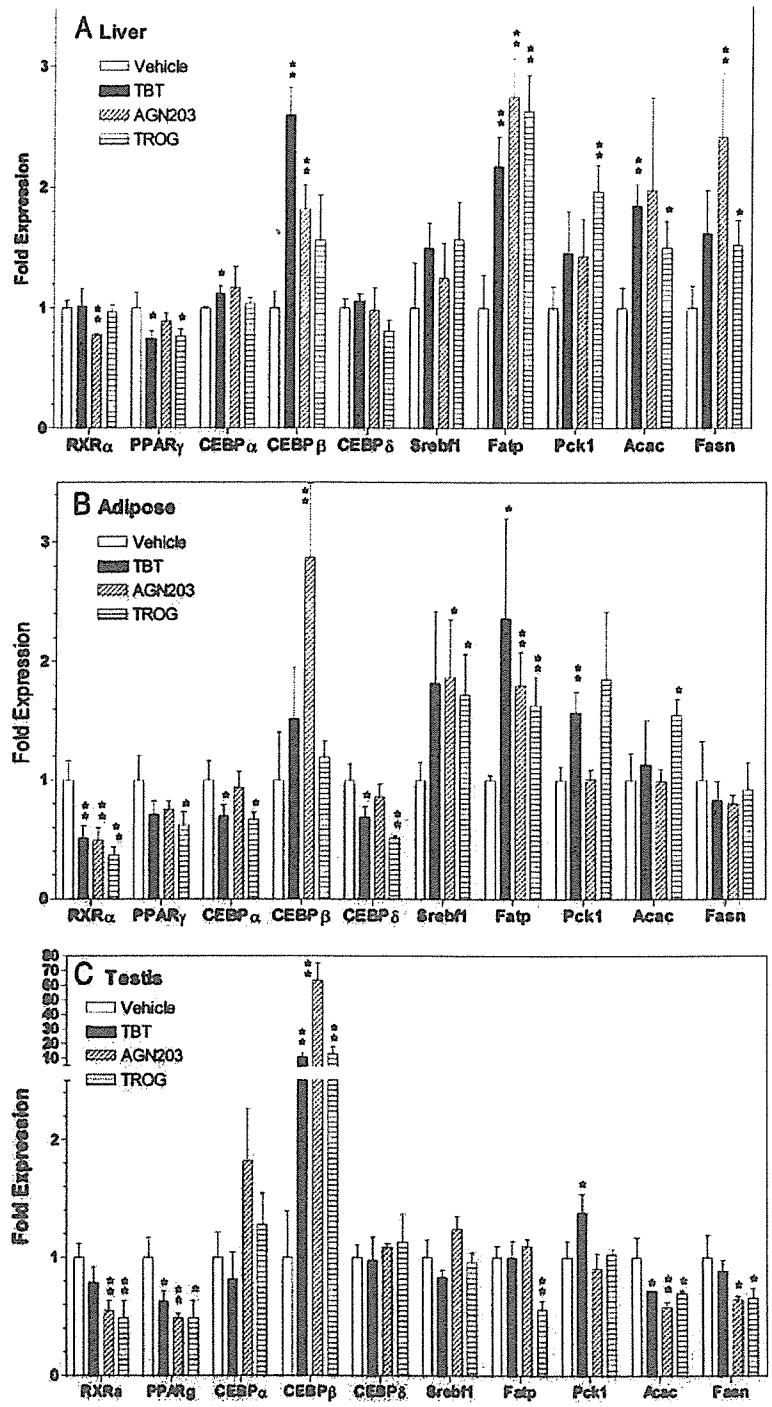

Fig. 3. *In Vivo* Induction of Adipogenic Modulators and RXR:PPARγ Target Genes

C57BL/6 male mice (three animals per treatment) were dosed with TBT (0.3 mg/kg b.w.), AGN195203 (0.3 mg/kg), troglitazone (3 mg/kg b.w.), or vehicle (corn oil) only by ip injection. Animals were killed after 24 h and dissected and cDNA was prepared from liver, epididymal fat pad, or testis for quantitative real-time PCR analysis. Expression levels were normalized to histone Hist2h4 and shown as the average fold change ± SEM (n = 3) compared with vehicle (corn oil) controls. Control *vs.* ligand treatments were analyzed by the unpaired Student's *t* test: *, $P < 0.1$; **, $P < 0.05$. TROG, Troglitazone.

with Oil Red O to assess changes in total tissue lipid accumulation. TBT exposure caused a disorganization of hepatic (Fig. 4, A and B) and gonadal (Fig. 4, C and D) architecture and significantly increased Oil Red O staining in treated animals *vs.* controls. Liver sections exhibited signs of steatosis consistent with the mis-

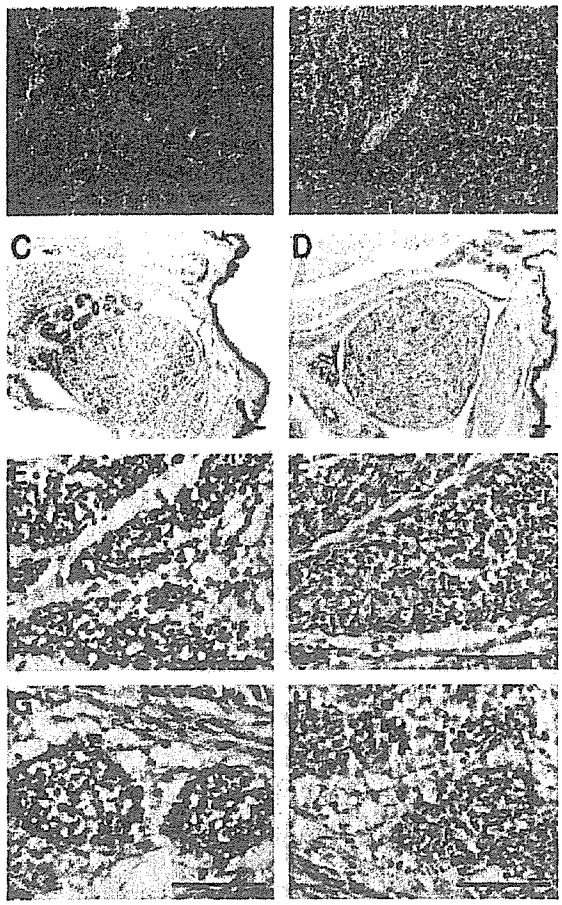

Fig. 4. *In Utero* Exposure to TBT Increases Adiposity in Mouse Liver, Testis, and Adipose Depots

Histological sections (12 μm) of newborn mouse liver (A and B), testis (C and D), inguinal adipose (E and F) and mammary adipose (G and H) stained with Oil Red O and counterstained with hematoxylin following *in utero* exposure to vehicle only (sesame oil) (A, C, E, and G) or 0.5 mg/kg b.w. TBT (B, D, F, and H) given s.c. daily from E12–18. *Scale bar*, 100 μm.

regulation of fatty acid uptake and synthesis observed using molecular markers. In addition, Oil Red O positive staining in mammary and inguinal adipose (Fig. 4, E–H) tissues was dramatically elevated, reflecting either an increase in lipid accumulation or an increase in mature adipocytes.

To determine whether exposure induced long-term changes in growth or adipose tissue, we followed mice from birth to adulthood after *in utero* exposure to TBT as indicated above. At birth, mice were cross-fostered to unexposed dams, and total body weight was recorded until 10 wk of age (Fig. 5A). Growth curves for male and female pups showed a slight trend for lower total body weight consistent with published observations (9) but were not statistically significant at 10 wk [control *vs.* TBT: male, 26.00 g ± 0.70 (n = 9) *vs.* 25.53 g ± 0.39 (n = 10), $P = 0.583$; female, 21.22 g ± 0.41 (n = 10), *vs.* 20.24 g ± 0.24 (n = 10), $P = 0.0529$]. Males were killed at 10 wk and epididymal fat pads were weighed (Fig. 5B). Adipose mass in TBT-treated males was increased significantly by 20% over controls [control *vs.* TBT: 0.30 g ± 0.020 (n = 9) *vs.* 0.36 g ± 0.018 (n = 10), $P = 0.0374$]. These data support the conclusion that TBT can increase body adiposity without overtly increasing total body weight. Similar lipid accumulation and changes in adipose tissue mass have also been observed after TZD or rexinoid treatment (55–57).

We had previously observed that TBT activated *Xenopus* RXRs (Table 1) and reasoned that the strong conservation in vertebrate nuclear receptor signaling pathways should result in consistent responses to organotin and RXR/PPARγ ligands across diverse vertebrate species. We therefore tested chronic exposure to environmentally relevant low doses of TBT (1–10 nM), the RXR-specific ligands LG100268 and AGN195203 (10–100 nM), troglitazone (0.1–1 μM), and estradiol (1–10 nM) on developing *X. laevis* tadpoles from stage 48 to metamorphs. To determine the effectiveness of these doses in *X. laevis* tadpoles, we used aromatase expression as a molecular marker because activity and expression are sensitive to endocrine disruption by organotins and RXR/PPARγ ligands in mammals (17, 18). *Xenopus* aromatase expression was similarly repressed 2- to 3-fold by 10 nM TBT, AGN195203, LG100268, or 1 μM troglitazone at stage 56 tadpoles (Fig. 6A) and at all subsequent stages. Despite significant ligand-induced aromatase down-regulation, neither sex ratios nor the time required to reach metamorphosis was altered (data not shown). *Xenopus* liver and kidney also exhibited no gross structural abnormalities at the doses given.

However, consistent with the testis and adipose results from mice presented above, we observed a dose-dependent increase in ectopic adipocyte formation posterior to the fat bodies in and around the gonads of both sexes after TBT or RXR/PPARγ ligand exposure (Fig. 6B). In contrast, estradiol-treated animals did not show increased adipocyte formation compared with controls. At 10 nM TBT, 10 nM AGN195203, or 1 μM troglitazone, ectopic adipocytes were observed in approximately 45–60% of animals. At the highest dose of TBT in males, testicular tissue was interspersed with, or replaced by, adipocytes along the anterior-posterior axis (Fig. 6, D, E, and G).

The concordant changes observed in *Xenopus* aromatase expression, gonadal adipocyte formation, and increased murine adiposity after exposure to TBT, RXR and PPARγ ligands are therefore consistent with a common mechanism of action through RXR:PPARγ activation, supporting the conclusion that endocrine disruption via nuclear receptor transcriptional regulation is a novel and key feature of organotin toxicity.

DISCUSSION

We have shown above that TBT is a potent inducer of adipogenesis, *in vitro* and *in vivo*, by acting as a novel,

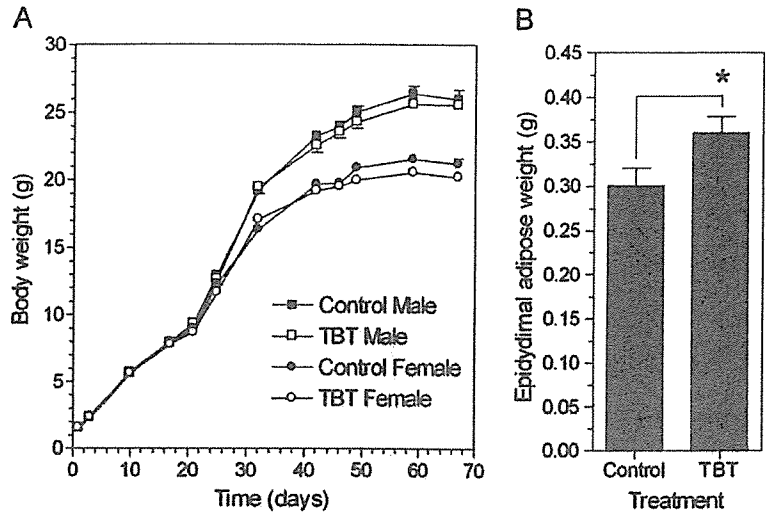

Fig. 5. *In Utero* Exposure to TBT Increases Adipose Mass But Not Body Weight in Adult Mice

A, Growth curves of C57BL/6 male and female pups exposed to control (sesame oil) or TBT *in utero* (E12–18). Data are mean ± SEM (n = 10). B, Epididymal fat pad weights from control or TBT-treated males at 10 wk. *, Epididymal adipose mass from exposed males was approximately 20% greater [control *vs.* TBT: 0.30 g ± 0.020 (n = 9) *vs.* 0.36 g ± 0.018 (n = 10); *, $P = 0.0374$). Data represent mean ± SEM (n = 9–10).

high-affinity xenobiotic ligand for RXRα and PPARγ. The ability of organotins to bind and activate these receptors, in particular the RXRs, which exhibit very restricted ligand specificity, is unexpected given the radically different chemical composition and three-dimensional molecular structure of organotins when compared with known natural and synthetic nuclear receptor ligands. Typically, RXR ligands comprise a carboxylic acid functional group and a three-dimensional molecular shape that mimics 9-*cis* RA. Structure-activity profiles indicate distinct structural preferences for organotins but also a relatively broad accommodation for agonist activity that is not easily reconciled with the classical ligand-binding model. Organotins may therefore interact somewhat differently than previously described RXR/PPARγ ligands with receptor LBDs to induce productive conformational changes required for coactivator recruitment. However, the binding data indicate that TBT is a potent and efficacious ligand for both RXRs and PPARγ that interacts, at least partially, with the same receptor-binding sites of other high-affinity ligands and promotes the necessary cofactor interactions required for agonist activation. In the study of Kanayama *et al.* (24), TBT was only effective in coactivator recruitment assays with PPARγ above 10 μM *in vitro*. However, in accord with our findings, they show that TBT activated PPARγ significantly at nanomolar concentrations in transfection assays. This may reflect a limitation of preference in the cofactor used *in vitro*. Alternatively, the lower maximal activation observed with TBT on PPARγ in cells (~30% at 100 nM TBT cf troglitazone) is consistent with one of two possibilities: either nonspecific cellular toxicity at high levels or activation as a partial agonist.

The ability of TBT to act as a dual ligand for permissive heterodimers such as RXRα:PPARγ, which can be activated by specific ligands for either receptor, also raises the possibility for additive or synergistic effects that might increase the potency of these compounds *in vivo* at low doses for this specific signaling pathway. Of note is that receptor activation is observed at nanomolar concentrations, whereas other mechanisms of toxicity and endocrine disruption, *e.g.* direct inhibition of aromatase activity, typically occur in the micromolar range. Furthermore, the activation of other permissive RXR heterodimeric partners, *e.g.* LXR and NURR1, suggests that organotins may act more widely to disrupt multiple nuclear receptor-mediated hormonal signaling pathways.

The biological consequences of organotin activation of the RXR:PPARγ signaling pathway are predictable and should follow known aspects of RXR/PPARγ biology. The RXR:PPARγ pathway plays a key role in adipocyte differentiation and energy storage, and is central to the control of whole-body metabolism (58). PPARγ activation increases the expression of genes that promote fatty acid storage and represses genes that induce lipolysis in adipocytes in white adipose tissue (59). PPARγ such as the thiazolidinediones can modulate insulin sensitivity due to these effects on the adipocyte, reversing insulin resistance in the whole body by sensitizing the muscle and liver tissue to insulin (60). However, a consequence of this increase in whole-body insulin sensitivity is that fat mass is increased through the promotion of triglyceride storage in adipocytes. Evidence is also mounting that depot-specific remodeling and adipocyte numbers increase after thiazolidinedione treatment (55–57). Therefore, PPARγ agonists comprise a class of phar-

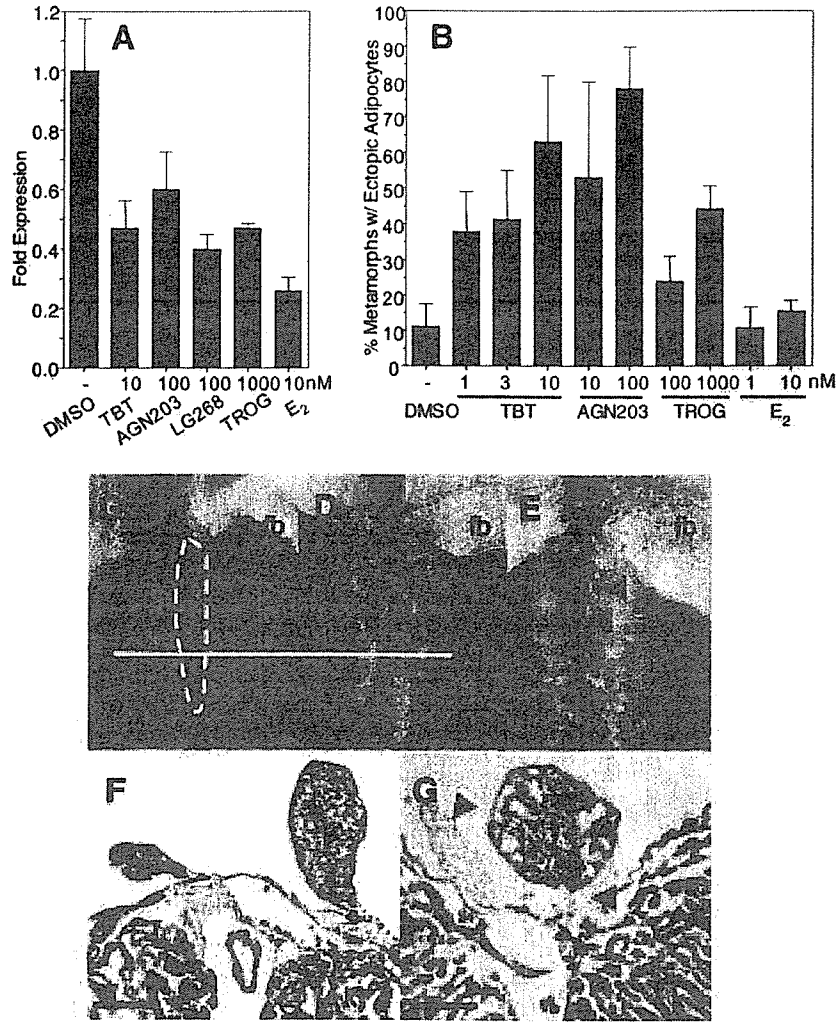

Fig. 6. Endocrine Disruption of RXR:PPARγ Signaling and Ectopic Induction of Adipocytes in *X. laevis* by TBT

A, Expression levels of *Xenopus* aromatase (XCYP19) were determined in tadpoles (stage 56) by quantitative real-time PCR after 24-h exposure to vehicle only (DMSO) or the indicated ligands. Expression was normalized to *Xenopus* EF1α and expressed as average fold change in expression ± SEM (n = 9) relative to vehicle controls. B, *X. laevis* tadpoles were dosed weekly under static renewal conditions with indicated ligands from stage 48 (before gonadogenesis) until stage 64 (metamorphic climax). Metamorphs (stage 66) were scored for ectopic adipocyte patches on gonads and urogenital ducts. Data are shown as the percentage of metamorphs exhibiting ectopic adipocyte patches posterior to the fat bodies; mean ± SD from triplicate tanks. C–E, Dissecting microscope photographs of kidneys (k), testis (t), and fat bodies (fb) from DMSO control, 10 nM TBT, and 1 μM troglitazone-treated male metamorphs. Multiple ectopic adipocyte patches (*red arrows*) are present posterior to the fat bodies along the anterior-posterior axis of gonads in TBT (D)- and troglitazone (E)-treated animals but not controls (C). Histological sections of kidneys and gonads from the same control (F) and 10 nM TBT (G)-treated males at the level indicated by the *white line* in C and D. Gonadal and connective tissue was either completely replaced by, or interspersed with, adipocytes (*red arrows*) in TBT-treated animals. Sections were developed with Mallory's trichrome stain. *Scale bars*, 100 μm.

maceutical therapies for type 2 diabetes that can also promote obesity by increasing fat storage. Likewise, RXR ligands also act as insulin-sensitizing agonists in rodents (61), underscoring the permissive nature of the PPARγ:RXR heterodimer and the potential effects on diabetes and obesity of both PPARγ and RXR agonists.

Our data are consistent with recent studies that organotins can mediate some of their endocrine disruption effects by transcriptional regulation through nuclear receptors, in particular RXR:PPARγ signaling (17–19, 24). Consequently, TBT exposure can promote adipocyte differentiation in the same manner as other RXR or PPARγ ligands *in vitro* using the standard murine 3T3-L1 cell model and *in vivo* through increased adiposity after intrauterine organotin exposure in newborn mice. It is currently unknown whether the increased adiposity *in vivo* results from an increase

in adipocyte precursor cell number, enhanced adipocyte differentiation from the same number of precursors, an increase in adipocyte size without an increase in number, or some combination of these.

The prevailing epidemiological data ascribe high-density caloric and/or fatty diets coupled with decreased physical activity as the root causes for the rise in obesity rates in the general population (62). The contribution of genetic components is less clear. Although genetic variation contributes to an individual's propensity to develop obesity, the rapid worldwide increase in obesity suggests that interaction with the modern environment exposes inherent genetic differences. The Barker hypothesis postulates that *in utero* fetal nutritional status is a potential risk factor for metabolic syndrome diseases (63–67). In this view, developmental metabolic programming of a thrifty phenotype limits the range in adaptive responses to the environment, *e.g.* diet and exercise, in later life (68). Experimental evidence from animal models lends support to this hypothesis (69). Plausible mechanisms include imprinting of obesity-sensitive hormonal pathways or changes in cell type and number, *e.g.* adipocytes, established during development.

Others, however, argue that the environment plays another role in obesity. Because the increase in obesity rates parallels the rapid growth in the use of industrial chemicals over the past 40 yr, it is plausible and provocative to associate *in utero* or chronic lifetime exposure to chemical triggers present in the modern environment with this epidemic. Hence, an "obesogen" model predicts the existence of xenobiotic chemicals that inappropriately regulate lipid metabolism and adipogenesis to promote obesity. Several recent studies serve as proof-of-principle for such a hypothesis. Environmental estrogens such as bisphenol A and nonylphenol, for instance, can promote adipocyte differentiation or proliferation in murine cell lines (70, 71). Furthermore, epidemiological studies link maternal smoking during pregnancy to an elevated risk of childhood obesity (72–76).

Seen in this context, we propose that organotins such as TBT and its congeners are chemical stressors or obesogens that activate RXR:PPARγ signaling to promote long-term changes in adipocyte number and/or lipid homeostasis after developmental or chronic lifetime exposure.

MATERIALS AND METHODS

Plasmids and Transfections

pCMX-GAL4 and pCMX-VP16 plasmid fusion constructs to nuclear receptor LBDs and coactivators [GAL4-hRARα, hRXRα, -xRXRα/γ, -hPPARγ, -mPPARα, -human steroid and xenobiotic receptor (SXR), -NURR1, -VDR, -LXR, -hACTR, -hPPAR-binding protein (PBP), -human steroid receptor coactivator-1 (SRC-1), human transcriptional intermediary factor 2 (TIF2)] have been previously described (77–82). Transfections were performed in Cos7 cells (transformed green monkey kidney fibroblast cell line) essentially as described elsewhere (83) using MH200-x4-TK-Luc as reporter and normalized to pCMX-β-galactosidase controls. Briefly, Cos7 cells were seeded at 5000 cells per well in 96-well tissue culture plates in 10% fetal bovine serum/DMEM and transfected for 8 h with 11 μg/plate of DNA/calcium phosphate precipitate mix (MH200x4-TK-Luc-CMX-β-galactosidase-nuclear receptor/coactivator effector(s) at a ratio of 5:5:1). Cells were washed free of precipitate with PBS and media were replaced with serum-free insulin, transferrin, lipid, bovine serum albumin supplemented (ITLB)/DMEM (84) plus ligands for an additional 24 h before assays for luciferase and β-galactosidase activity. All transfection data points were performed in triplicate, and all experiments were repeated at least three times.

Quantitative Real-Time PCR Analyses

Total cellular RNA from C57BL/6 mouse and *X. laevis* tissues was isolated with Trizol reagent and reversed transcribed with oligo dT and Superscript II (Invitrogen, San Diego, CA) according to the manufacturer's instructions. Triplicate cDNA samples (50 ng/reaction) were analyzed by quantitative real-time PCR on a DNA Engine Opticon thermal cycler [MJ Research (Watertown, MA)/Bio-Rad Laboratories (Hercules, CA)] using SYBR Green chemistry (PerkinElmer Life Sciences, Wellesley, MA). Fold changes in expression levels were calculated after normalization to histone Hist2h4 using the Δ-Δ cycle threshold method (85). Gene-specific primers were as follows. Hist2h4 forward (F): 5′-CCCGTGGTGTGCTGAAGGTGTT-3′; reverse (R), 5′-GAATTGAAGCGGCGGCGTCTA-3′; RXRα F: 5′-CGGCTGCTCAGGGTACTTGTGTTT-3′; R, 5′-CGGCTGCTCAGGGTACTTGTGTTT-3′; PPARγ F: 5′-TGGGTGAAACTCTGGGAGATTC-3′; R, 5′-AATTTCTTGTGAAGTGCTCATAGGC-3′; C/EBPα F: 5′-CCAAGAAGTCGGTGGACAAGA-3′; R, 5′-CGGTCATTGTCACTGGTCAACT-3′; C/EBPβ F: 5′-GCCCGCCGCCTTTAGACC-3′; R, 5′-CGCTCGTGCTCGCCAATG-3′; C/EBPδ F: 5′-AACCCGCGGCCTTCTACGAG-3′; R, 5′-ACGGCGGCCATGGAGTCAAT-3′; aP2 F: 5′-GAATTCGATGAAATCACCGCA-3′; R, 5′-CTCTTTATTGTGGTCGACTTTCCA-3′; FATP F: 5′-AGCCGCTTCTGGGATGACTGTGT-3′; R, 5′-ACCGAAGCGCTGCGTGAACTC-3′; ACS F: 5′-CCCAGCCAGTCCCCACCAG-3′; R, 5′-CACACCACTCAGGCTCACACTCGT-3′; FASN F: 5′-TCGGGTGTGGTGGGTTTGGTGAAT-3′; R, 5′-ACTTGGGGGCGTGAGATGTGTTGC-3′;ACAC F: 5′-G GATGGCAGCTCTGGAGGTGTATG-3′; R, 5′-TGTCCTTAAGCTGGCGGTGTTGTA; Pck1 F: 5′-CTGGCAGCATGGGGTGTTTGTAGG-3′; R, 5′-TGCCGAAGTTGTAGCCGAAGAAGG-3′; Srebf1 F: 5′-GCCCCTGCCCACCTCAAACCT-3′; R, 5′-ACTGGCACGGGCATCCTTCCTC-3′; *Xenopus* EF1α F: 5′-GATCCCAGGAAAGCCAATGTGC 3′; R, 5′-CCGGATCCTGCTGCCTTCTTCT-3′; *Xenopus* CYP19 (aromatase) F: 5′-GTCTGGATTAATGGCGAGGAAACA-3′; R, 5′-CTGATGAAGTATGGCCGAATGACC-3′.

Ligand Binding

Histidine-tagged RXRα LBD (H_6-RXRα LBDs) was expressed and purified from pET15b(+) vector in BL21(DE3) pLysS bacteria cultures after induction with 1 mM isopropyl-β-D-thiogalactopyranoside for 3 h at 37 C (86). Purified H_6-PPARγ was purchased from Invitrogen. Proteins were bound to 96-well Nickel Chelate Flashplates (PerkinElmer Life Sciences) at 100 μg/ml overnight at 4 C and washed five times with 200 μl/well Flashplate Assay Buffer (20 mM HEPES, pH 7.9; 100 mM KCl, 0.1% cholamidopropyldimethylammonio-2-hydroxy-1-propanesulfonate, 0.1 mM dithiothreitol). Competition assays typically used 1–5 nM [^{3}H]-9-*cis*-RA (PerkinElmer Life Sciences) or 10–50 nM [^{3}H]rosiglitazone (American Radiochemicals, Inc., St. Louis, MO) plus cold competitor ligands in Flashplate Assay Buffer at concentrations indicated in the figures. Plates were incubated at room temperature, pro-

tected from light, and read after 4 h on a Packard Topcount scintillation counter (Packard Instruments, Meriden, CT). Specific bound counts/min were determined by subtraction of counts/min from uncoated wells at each ligand concentration. Data were analyzed with GraphPad Prism 4.0 (GraphPad Software, Inc., San Diego, CA) using a one-site competition binding equation to determine K_i values for competitor ligands; K_d values of 1.4 and 41 nM for 9-*cis*-RA and rosiglitazone for their respective receptors were used in the calculations (87, 88).

3T3-L1 Cell Assays

3T3-L1 (American Type Culture Collection, Manassas, VA) cells were maintained as subconfluent cultures by passage every 3 d from cultures seeded at 5000 cells/cm^2 in 8% calf serum/DMEM. For differentiation assays, cells were seeded at 15×10^3 cells per well into 24-well tissue culture plates in 8% fetal bovine serum/DMEM, after which cultures were grown for 2 d and then treated with the indicated RXR, RAR, and PPAR ligands either with or without MDIT (100 μM 3-isobutyl-1-methylxanthine, 100 nM dexamethasone, 0.1 ng/ml insulin, and 2 nM T_3 thyroid hormone) induction cocktail. Media and ligand treatments were renewed every 2 d. After 1 wk, cells were scored for adipocyte differentiation by Oil Red O staining for lipid droplet accumulation. Cultures were washed with PBS, fixed with 10% formaldehyde for 15 min, washed with distilled water, and stained with filtered Oil Red O solution (4 g/liter, 60% isopropanol) for 15 min. Excess stain was removed by washing three times with distilled water. Three random fields from each well were photographed under phase contrast and analyzed in ImageJ. Images were converted into high-contrast black and white images to visualize lipid droplets and scored as the percentage area per field. Data are shown as the mean ± SEM from three wells per treatment. The method was validated by extraction of Oil Red O from stained cells into 100% isopropanol and quantitated by absorbance at 540 nm on a spectrophotometer.

In Vivo Animal Exposure Experiments

C57BL/6J mice were housed under a 12-h light, 12-h dark cycle. Pregnant mice were dosed by ip injection with TBT [0.05 or 0.5 mg/kg body weight (b.w.)] or vehicle (sesame oil) from embryonic d 12 (E12) every 24 h until the day before delivery. Neonates were killed at the day of delivery and analyzed. The samples were embedded in optimal cutting temperature embedding compound and sectioned (12 mm) using a cryostat. Sections were fixed on slides with 4% paraformaldehyde for 10 min and rinsed in PBS. The slides were then sequentially washed with distilled water and 60% of isopropanol and stained with Oil Red O (4 g/liter, 60% isopropanol). After washing with 60% isopropanol and distilled water, the slides were counterstained with hematoxylin. Sections were evaluated and photographed using a Zeiss microscope (Carl Zeiss, Thornwood, NY).

For long-term growth studies, pups were cross-fostered to unexposed C57BL/6 dams after birth, and litter sizes were kept constant at eight pups per dam (control, two male + two female; TBT treated, two male + two female). Animals were weaned at 3 wk of age and maintained on standard rodent chow. Total body weight was followed until 10 wk of age. Males were then killed, and epididymal fat pads were dissected and weighed.

X. laevis tadpoles were sorted at stage 48 (89) and maintained in 1-liter glass tanks in 20% Holtfreter's buffered salt solution (90) at a density of 10 tadpoles per tank on a diet of ground Tetramin Fish Flakes and spirulina. Compounds prepared in dimethylsulfoxide (DMSO) as 10^5-fold stock solutions were tested on triplicate tanks and dosed by static renewal after weekly water changes. Metamorphs at stage 64 were transferred to individual containers and fed frozen brine shrimp for 2 wk until stage 66. Froglets were euthanized with 250 mg/liter MS222 in 20% Holtfreter's solution and then scored for gonadal abnormalities and interrenal/gonadal adipocyte formation under a dissecting microscope. Kidneys with attached gonads and livers were fixed in 10% formalin-PBS, embedded in paraffin, and sectioned at 15 μm thickness. Sections were developed with Mallory's trichrome stain.

All animal experiments were approved and performed in accordance with Institutional Animal Care and Use Committee protocols.

Acknowledgments

We thank Drs. I. Blitz, K. Cho, C. Zhou, and T. Osborne for critical reading and comments on the manuscript, Dr. C. Li (Expression Technologies) for the H_6-RXRα LBD construct, and Dr. R. Chandraratna (Allergan Pharmaceuticals, Irvine, CA) for AGN203 and LG268).

Received September 8, 2005. Accepted March 30, 2006.

Address all correspondence and requests for reprints to: Bruce Blumberg, Department of Developmental and Cell Biology, University of California Irvine, 2113 McGaugh Hall, Irvine, California 92697-2300. E-mail: blumberg@uci.edu.

This work was supported by grants from the U.S. Environmental Protection Agency (STAR R830686) and National Institutes of Health (GM-60572) (to B.B.); from the Ministries of Education, Culture, Sports, Science and Technology, Environment and Health Labor and Welfare, Japan (to T.I.); and from the University of California Toxic Substance Research and Training Program (UC-37579) (to F.G.).

F.G., H.W., Z.Z., L.M., K.A., R.C., D.M.G., J.K., T.I. have nothing to declare. B.B. is a named inventor on U.S. patents US 5,861,274, US 6,200,802, and US 6,815,168.

REFERENCES

1. Appel KE 2004 Organotin compounds: toxicokinetic aspects. Drug Metab Rev 36:763–786
2. Golub M, Doherty J 2004 Triphenyltin as a potential human endocrine disruptor. J Toxicol Environ Health B Crit Rev 7:281–295
3. Blaber SJM 1970 The occurrence of a penis-like outgrowth behind the right tentacle in spent females of *Nucella lapillus*. Proc Malacolog Soc London 39:231–233
4. Gibbs P, Bryan G 1986 Reproductive failure in populations of the dog-whelk, *Nucella lapillus*, caused by imposex induced by tributyltin from antifouling paints. J Mar Biol Assoc UK 66:767–777
5. Matthiessen P, Gibbs P 1998 Critical appraisal of the evidence for tributyltin-mediated endocrine disruption in mollusks. Environ Toxicol Chem 17:37–43
6. Shimasaki Y, Kitano T, Oshima Y, Inoue S, Imada N, Honjo T 2003 Tributyltin causes masculinization in fish. Environ Toxicol Chem 22:141–144
7. McAllister BG, Kime DE 2003 Early life exposure to environmental levels of the aromatase inhibitor tributyltin causes masculinisation and irreversible sperm damage in zebrafish (*Danio rerio*). Aquat Toxicol 65:309–316
8. Omura M, Ogata R, Kubo K, Shimasaki Y, Aou S, Oshima Y, Tanaka A, Hirata M, Makita Y, Inoue N 2001 Two-generation reproductive toxicity study of tributyltin chloride in male rats. Toxicol Sci 64:224–232
9. Ogata R, Omura M, Shimasaki Y, Kubo K, Oshima Y, Aou S, Inoue N 2001 Two-generation reproductive toxicity

study of tributyltin chloride in female rats. J Toxicol Environ Health A 63:127–144
10. Boyer IJ 1989 Toxicity of dibutyltin, tributyltin and other organotin compounds to humans and to experimental animals. Toxicology 55:253–298
11. Heidrich DD, Steckelbroeck S, Klingmuller D 2001 Inhibition of human cytochrome P450 aromatase activity by butyltins. Steroids 66:763–769
12. Cooke GM 2002 Effect of organotins on human aromatase activity in vitro. Toxicol Lett 126:121–130
13. Powers MF, Beavis AD 1991 Triorganotins inhibit the mitochondrial inner membrane anion channel. J Biol Chem 266:17250–17256
14. Gennari A, Viviani B, Galli CL, Marinovich M, Pieters R, Corsini E 2000 Organotins induce apoptosis by disturbance of [Ca(2+)](i) and mitochondrial activity, causing oxidative stress and activation of caspases in rat thymocytes. Toxicol Appl Pharmacol 169:185–190
15. Philbert MA, Billingsley ML, Reuhl KR 2000 Mechanisms of injury in the central nervous system. Toxicol Pathol 28:43–53
16. Mu YM, Yanase T, Nishi Y, Waseda N, Oda T, Tanaka A, Takayanagi R, Nawata H 2000 Insulin sensitizer, troglitazone, directly inhibits aromatase activity in human ovarian granulosa cells. Biochem Biophys Res Commun 271:710–713
17. Mu YM, Yanase T, Nishi Y, Takayanagi R, Goto K, Nawata H 2001 Combined treatment with specific ligands for PPARγ:RXR nuclear receptor system markedly inhibits the expression of cytochrome P450arom in human granulosa cancer cells. Mol Cell Endocrinol 181:239–248
18. Saitoh M, Yanase T, Morinaga H, Tanabe M, Mu YM, Nishi Y, Nomura M, Okabe T, Goto K, Takayanagi R, Nawata H 2001 Tributyltin or triphenyltin inhibits aromatase activity in the human granulosa-like tumor cell line KGN. Biochem Biophys Res Commun 289:198–204
19. Nishikawa J, Mamiya S, Kanayama T, Nishikawa T, Shiraishi F, Horiguchi T 2004 Involvement of the retinoid X receptor in the development of imposex caused by organotins in gastropods. Environ Sci Technol 38: 6271–6276
20. Baillie-Hamilton PF 2002 Chemical toxins: a hypothesis to explain the global obesity epidemic. J Altern Complement Med 8:185–192
21. Heindel JJ 2003 Endocrine disruptors and the obesity epidemic. Toxicol Sci 76:247–249
22. Jacobs MN, Lewis DF 2002 Steroid hormone receptors and dietary ligands: a selected review. Proc Nutr Soc 61:105–122
23. Watanabe H, Iguchi T, Morohashi K 2002 [Endocrine disruptors and nuclear receptors]. Nippon Rinsho 60: 397–403
24. Kanayama T, Kobayashi N, Mamiya S, Nakanishi T, Nishikawa J 2005 Organotin compounds promote adipocyte differentiation as agonists of the peroxisome proliferator-activated receptor γ/retinoid X receptor pathway. Mol Pharmacol 67:766–774
25. Wang Z, Benoit G, Liu J, Prasad S, Aarnisalo P, Liu X, Xu H, Walker NP, Perlmann T 2003 Structure and function of Nurr1 identifies a class of ligand-independent nuclear receptors. Nature 423:555–560
26. Aarnisalo P, Kim CH, Lee JW, Perlmann T 2002 Defining requirements for heterodimerization between the retinoid X receptor and the orphan nuclear receptor Nurr1. J Biol Chem 277:35118–35123
27. Boehm MF, Zhang L, Zhi L, McClurg MR, Berger E, Wagoner M, Mais DE, Suto CM, Davies JA, Heyman RA, Nadzant AM 1995 Design and synthesis of potent retinoid X receptor selective ligands that induce apoptosis in leukemia cells. J Med Chem 38:3146–3155
28. Yu C, Chen L, Luo H, Chen J, Cheng F, Gui C, Zhang R, Shen J, Chen K, Jiang H, Shen X 2004 Binding analyses between human PPARγ-LBD and ligands. Eur J Biochem 271:386–397
29. Forman BM, Tontonoz P, Chen J, Brun RP, Spiegelman BM, Evans RM 1995 15-Deoxy-δ 12, 14-prostaglandin J2 is a ligand for the adipocyte determination factor PPAR γ. Cell 83:803–812
30. Schoonjans K, Staels B, Auwerx J 1996 The peroxisome proliferator activated receptors (PPARs) and their effects on lipid metabolism and adipocyte differentiation. Biochim Biophys Acta 1302:93–109
31. Kersten S 2002 Peroxisome proliferator activated receptors and obesity. Eur J Pharmacol 440:223–234
32. Lane MD, Tang QQ, Jiang MS 1999 Role of the CCAAT enhancer binding proteins (C/EBPs) in adipocyte differentiation. Biochem Biophys Res Commun 266:677–683
33. Tang QQ, Otto TC, Lane MD 2003 CCAAT/enhancer-binding protein β is required for mitotic clonal expansion during adipogenesis. Proc Natl Acad Sci USA 100: 850–855
34. Tang QQ, Lane MD 1999 Activation and centromeric localization of CCAAT/enhancer-binding proteins during the mitotic clonal expansion of adipocyte differentiation. Genes Dev 13:2231–2241
35. Rubin CS, Hirsch A, Fung C, Rosen OM 1978 Development of hormone receptors and hormonal responsiveness in vitro. Insulin receptors and insulin sensitivity in the preadipocyte and adipocyte forms of 3T3–L1 cells. J Biol Chem 253:7570–7578
36. Kletzien RF, Clarke SD, Ulrich RG 1992 Enhancement of adipocyte differentiation by an insulin-sensitizing agent. Mol Pharmacol 41:393–398
37. Kletzien RF, Foellmi LA, Harris PK, Wyse BM, Clarke SD 1992 Adipocyte fatty acid-binding protein: regulation of gene expression in vivo and in vitro by an insulin-sensitizing agent. Mol Pharmacol 42:558–562
38. Tafuri SR 1996 Troglitazone enhances differentiation, basal glucose uptake, and Glut1 protein levels in 3T3–L1 adipocytes. Endocrinology 137:4706–4712
39. Xue JC, Schwarz EJ, Chawla A, Lazar MA 1996 Distinct stages in adipogenesis revealed by retinoid inhibition of differentiation after induction of PPARγ. Mol Cell Biol 16:1567–1575
40. Kawada T, Kamei Y, Sugimoto E 1996 The possibility of active form of vitamins A and D as suppressors on adipocyte development via ligand-dependent transcriptional regulators. Int J Obes Relat Metab Disord 20(Suppl 3):S52–S57
41. Kawada T, Kamei Y, Fujita A, Hida Y, Takahashi N, Sugimoto E, Fushiki T 2000 Carotenoids and retinoids as suppressors on adipocyte differentiation via nuclear receptors. Biofactors 13:103–109
42. Tontonoz P, Graves RA, Budavari AI, Erdjument-Bromage H, Lui M, Hu E, Tempst P, Spiegelman BM 1994 Adipocyte-specific transcription factor ARF6 is a heterodimeric complex of two nuclear hormone receptors, PPAR γ and RXR α. Nucleic Acids Res 22:5628–5634
43. Martin G, Schoonjans K, Lefebvre AM, Staels B, Auwerx J 1997 Coordinate regulation of the expression of the fatty acid transport protein and acyl-CoA synthetase genes by PPARα and PPARγ activators. J Biol Chem 272:28210–28217
44. Motojima K, Passilly P, Peters JM, Gonzalez FJ, Latruffe N 1998 Expression of putative fatty acid transporter genes are regulated by peroxisome proliferator-activated receptor α and γ activators in a tissue- and inducer-specific manner. J Biol Chem 273:16710–16714
45. Frohnert BI, Hui TY, Bernlohr DA 1999 Identification of a functional peroxisome proliferator-responsive element in the murine fatty acid transport protein gene. J Biol Chem 274:3970–3977
46. Martin G, Poirier H, Hennuyer N, Crombie D, Fruchart JC, Heyman RA, Besnard P, Auwerx J 2000 Induction of the fatty acid transport protein 1 and acyl-CoA synthase